Atmos. Chem. Phys. Discuss., 14, 26495–26543, 2014
www.atmos-chem-phys-discuss.net/14/26495/2014/
doi:10.5194/acpd-14-26495-2014

Atmospheric Chemistry and Physics Discussions

How emissions, climate, and land use change will impact mid-century air quality over the United States: a focus on effects at National Parks

M. Val Martin[1,2], C. L. Heald[3], J.-F. Lamarque[4], S. Tilmes[4], L. K. Emmons[4], and B. A. Schichtel[5,6]

[1]Atmospheric Science Department, Colorado State University, Fort Collins, CO, USA
[2]Chemical and Biological Engineering Department, The University of Sheffield, Sheffield, UK
[3]Department of Civil and Environmental Engineering, Massachusetts Institute of Technology, Cambridge, MA, USA
[4]National Center for Atmospheric Research, Boulder, CO, USA
[5]National Park Service, Fort Collins, CO, USA
[6]Cooperative Institute for Research in the Atmosphere, Fort Collins, CO, USA

Received: 3 October 2014 – Accepted: 6 October 2014 – Published: 22 October 2014

Correspondence to: M. Val Martin (m.valmartin@sheffield.ac.uk)

Published by Copernicus Publications on behalf of the European Geosciences Union.

Abstract

We use a global coupled chemistry-climate-land model (CESM) to assess the integrated effect of climate, emissions and land use changes on annual surface O_3 and $PM_{2.5}$ on the United States with a focus on National Parks (NPs) and wilderness areas, using the RCP4.5 and RCP8.5 projections. We show that, when stringent domestic emission controls are applied, air quality is predicted to improve across the US, except surface O_3 over the western and central US under RCP8.5 conditions, where rising background ozone counteracts domestic emissions reductions. Under the RCP4.5, surface O_3 is substantially reduced (about 5 ppb), with daily maximum 8 h averages below the primary US EPA NAAQS of 75 ppb (and even 65 ppb) in all the NPs. $PM_{2.5}$ is significantly reduced in both scenarios (4 $\mu g\,m^{-3}$; $\sim$ 50 %), with levels below the annual US EPA NAAQS of 12 $\mu g\,m^{-3}$ across all the NPs; visibility is also improved (10–15 deciviews; > 75 km in visibility range), although some parks over the western US (40–74 % of total sites in the US) may not reach the 2050 target to restore visibility to natural conditions by 2064. We estimate that climate-driven increases in fire activity may dominate summertime $PM_{2.5}$ over the western US, potentially offsetting the large $PM_{2.5}$ reductions from domestic emission controls, and keeping visibility at present-day levels in many parks. Our study suggests that air quality in 2050 will be primarily controlled by anthropogenic emission patterns. However, climate and land use changes alone may lead to a substantial increase in surface O_3 (2–3 ppb) with important consequences for O_3 air quality and ecosystem degradation at the US NPs. Our study illustrates the need to consider the effects of changes in climate, vegetation, and fires in future air quality management and planning and emission policy making.

1 Introduction

Air pollution, such as surface ozone (O_3) and fine particulate matter (with diameter < 2.5 µm; $PM_{2.5}$), has evolved in both urban and rural regions around the world over

ACPD
14, 26495–26543, 2014

the last centuries. Air pollution changes have resulted in part from direct changes in natural and anthropogenic emissions and in part from indirect changes in climate and land use (Jacob and Winner, 2009; Arneth et al., 2010; Fiore et al., 2012). A changing climate is projected to significantly modify both natural and anthropogenic emissions and the atmospheric processes that govern air pollution transport, transformation, and deposition. For example, a warming climate is expected to increase wildfires and associated emissions of trace gases and particulate matter (Spracklen et al., 2009; Yue et al., 2013), cause a general increase in biogenic emissions (Heald et al., 2008), and increase emissions of O_3 and aerosol precursors, such as nitrogen oxides (NO_x) and ammonia (NH_3), from soil and agricultural activities. Anthropogenic emissions are likely to change in response to economic, climatic, and political pressures and policies (IPCC, 2013). In addition, a changing climate is likely to alter precipitation and cloud patterns and synoptic-scale transport processes (Jacob and Winner, 2009). At the same time, changes in land cover and land use will influence the deposition of pollution, as well as the emission of O_3 and aerosol precursors (Ganzeveld et al., 2010; Wu et al., 2012). For example, deforestation decreases turbulent exchange and foliar uptake, prompting a rise in air pollutants. These effects may drive significant local increases or decreases in air pollution.

National Parks (NPs) and wilderness areas in the United States (US) are visited by millions of people every year to enjoy pristine nature. Maintaining adequate air quality conditions in these areas is key to preserving natural ecosystems, preventing negative impacts on visitor and staff health, and maximizing the beauty of landscapes. Air quality management in these regions, including efforts to develop meaningful emissions control strategies, relies on assessment of the current as well as future contributions of natural and anthropogenic sources to local air quality.

Two recent literature reviews (Jacob and Winner, 2009; Fiore et al., 2012) indicate that climate change alone will increase summertime surface ozone in polluted areas by 1–10 ppb. Pfister et al. (2014) predict an increase of about 5 ppb over the Rocky Mountain region during the summer in a future climate, with important potential results

ACPD
14, 26495–26543, 2014

to the US National Park Service for air quality management. Surface O_3 is toxic to humans and thus poses a threat to visitor and park staff health. In addition, accumulated exposure to elevated levels of O_3 can damage vegetation (e.g. Reich and Amundson, 1985; Schaub et al., 2005). Ozone levels have been shown to cause significant yield reduction in a number of major crops on a global scale (e.g. Avnery et al., 2011; Ghude et al., 2014), and in combination with warming may reduce global crop production by up to 15 % in 2050 (Tai et al., 2014), leading to substantial economic losses and potentially worsening global malnutrition. Studies have also reported many other negative impacts on ecosystems, such as reductions in tree and seedling growth, decreases in photosynthetic rates, and visible foliar injuries on multiple plant species, including broadleaf deciduous forest in the northeastern US and needleleaf evergreen forest in the western US (e.g. Arbaugh et al., 1998; Schaub et al., 2005). In addition, rising O_3 levels may substantially suppress the global land-carbon sink via its negative effect on the photosynthesis, leading to a greater accumulation of carbon dioxide in the atmosphere (Sitch et al., 2007).

Atmospheric fine particles are also harmful to human and ecosystem health. Short-term exposure to $PM_{2.5}$ can lead to respiratory illness such as asthma; longer-term exposure may result in more severe cardiovascular and respiratory diseases as well as lung cancer, increasing the risk of premature mortality (e.g. Pope and Dockery, 2006). Fine particles and gases cause haze, which degrades visibility. The importance of visibility at NPs and wilderness areas is recognized and protected by the US Environmental Protection Agency's (EPA) Regional Haze Rule (RHR), which establishes the goal of returning visibility to natural conditions. The RHR mandates that each state set "reasonable progress" goals to return visibility to natural conditions on the 20 % haziest days by 2064, while preventing further degradation of visibility on the 20 % clearest days (US EPA, 2003). Wild and prescribed fires are one of the primary contributors to air pollution, including haze-causing pollutants, in the western and southeastern US (e.g. Val Martin et al., 2013). Previous studies project that increased fire activity over the western United States will nearly double carbonaceous aerosol by 2050, and pro-

ACPD
14, 26495–26543, 2014

duce a significant increase in annual mean $PM_{2.5}$ and haze (Spracklen et al., 2009; Yue et al., 2013), exacerbating efforts to achieve "natural visibility".

In this study, we examine the integrated effect of climate change, anthropogenic emission changes, and land use change on air quality over the United States, with a particular focus on the US National Parks. To our knowledge, this is the first time that the relative effect of these three factors has been considered for US air quality projection. We use a global earth system model to estimate how surface O_3 and $PM_{2.5}$ are expected to change using two Representative Concentration Pathway (RCP) scenarios, represented in the IPCC (2013). We assess the changes in surface O_3 and $PM_{2.5}$ in 2050 relative to present-day levels and discuss the meteorological and chemical drivers behind these changes.

2 Modeling analysis

2.1 Model description and future changes

To simulate the impact of future changes on the US air quality, we use the Community Earth System Model (CESM) (http://www2.cesm.ucar.edu/). CESM is a global model, which includes atmospheric, land, ocean and sea ice models that can be run in standalone or coupled configurations. We run CESM version 1.1.1 with online computed meteorology and prescribed sea-surface and sea-ice distributions, corresponding to previous fully-coupled simulations. Simulations are performed at the horizontal resolution of $1.9^{\circ} \times 2.5^{\circ}$, and vertical resolution of 26 layers from the surface to about 4 hPa, with a time step of 30 min.

To simulate land processes, we use the Community Land Model (CLM) version 4 (Oleson et al., 2010). CLM describes the physical, chemical, and biological processes of terrestrial ecosystems, including the hydrology and carbon cycling of the terrestrial biosphere.

ACPD
14, 26495–26543, 2014

For the atmospheric model, we use the Community Atmospheric Model (CAM) version 4 (Neale et al., 2013) fully coupled with an interactive gas-aerosol scheme (CAM-Chem) (Lamarque et al., 2012). The chemical mechanism includes full tropospheric O_3–NO_x–CO–VOC and aerosol phase chemistry, based on the MOZART-4 chemical transport model (Emmons et al., 2010). Simulated aerosol mass classes include sulfate (SO_4), ammonium nitrate (NH_4NO_3), primary carbonaceous aerosols (black carbon, organic carbon), secondary organic aerosols (SOA), sea salt and dust. SO_4 is formed from the oxidation of SO_2 in the gas phase (by reaction with the hydroxyl radical) and in the aqueous phase (by reaction with ozone and hydrogen peroxide). NH_4NO_3 is determined from NH_3 emissions and the parameterization of gas/aerosol partitioning by Metzger et al. (2002), which is based on the level of sulfate present. Black carbon (BC) and organic carbon (OC) aerosols are directly emitted in a combination of hydrophobic and hydrophilic forms (80 and 50 % hydrophobic, respectively), and hydrophobic aerosol is converted to hydrophilic with a fixed 1.6 days e-folding time (Tie et al., 2005). Dust and sea salt are implemented following Mahowald et al. (2006a, b), with improvements from Albani et al. (2014); the sources of these natural aerosols are derived based on the model calculated wind speed and surface conditions. SOA are linked to the gas-phase chemistry through the oxidation of isoprene, monoterpenes, alkenes and toluene as in Lack et al. (2004). Finally, dry deposition is represented by the multiple resistance approach of Wesely (1989), with some updates (Emmons et al., 2010; Lamarque et al., 2012; Val Martin et al., 2014). The calculation of dry deposition velocities is performed in CLM and linked to land cover types. Therefore, dry deposition responds to changes in land cover and climate. In this work, we use the optimized dry deposition scheme described in Val Martin et al. (2014), in which the vegetation resistances are linked to the leaf area index (LAI). This optimized dry deposition scheme improves the simulation of O_3 dry deposition velocity, particularly over broadleaf forested regions, and significantly reduces the well-known, long lasting summertime surface O_3 bias over eastern US and Europe in CAM-Chem documented by Lamarque et al. (2012); we discuss this further in Sect. 2.2.

ACPD
14, 26495–26543, 2014

We perform time-slice experiments for 2000 (present-day and baseline) and 2050 (future), under the RCP scenarios designed in support of the IPCC AR5. The RCP include four scenarios, each of which corresponds to a specific pathway towards reaching a 2100 target radiative forcing (RF) (i.e., 2.6, 4.5, 6.0 and 8.5 Wm^{-2}) associated with greenhouse gases: RCP2.6, RCP4.5, RCP6.0 and RCP8.5, respectively. The RCP2.6 assumes a peak forcing (3.0 Wm^{-2}) in the early 21st century and a decline out to 2100, the RCP4.5 and RCP6.0 scenarios assume RF stabilization after 2100, and the RCP8.5 scenario assumes continuing growth in RF after 2100 (Moss et al., 2011). In this work, we select the RCP4.5 and RCP8.5 scenarios to bracket our results, i.e., we use a stabilization scenario (RCP4.5) and the largest forcing scenario (RCP8.5). Table 1 summarizes the main climate input data for 2000 and 2050. We apply monthly mean time varying sea-surface temperatures and sea-ice distributions generated by the Community Climate System Model, version 4 for the Coupled Model Intercomparison Project Phase 5 (Meehl et al., 2012). Our simulations also consider time varying, zonally averaged greenhouse gas distributions for CO_2, CH_4, N_2O and halogens, and future changes in stratospheric ozone levels.

Table 2 summarizes the main anthropogenic emissions for short-lived air pollutants and biogenic emissions projected over the United States. We divide the emissions for eastern and western US because of the different emission patterns. Emissions of NO_x, NH_3, CO, non-methane volatile organic compounds (VOCs), SO_2 and carbonaceous aerosols for anthropogenic activities and biomass burning are provided in 2000 by Lamarque et al. (2010) and in 2050 by the RCP database (van Vuuren et al., 2011, and references therein). Biomass burning emissions vary among the RCPs and in time, following changes in land cover and land use; however, they do not respond to changes in climate. Biogenic VOCs (e.g., isoprene and monoterpenes) are computed within CLM using the Model of Emissions of Gases and Aerosols from Nature (MEGAN2.1) algorithms (Guenther et al., 2012), and are allowed to respond interactively to temperature, light, soil moisture, leaf age and vegetation density (Heald et al., 2008). Both dust and seasalt are also emitted interactively in CESM (Mahowald et al., 2006a, b; Albani et al.,

ACPD
14, 26495–26543, 2014

2014). Other natural emissions of O_3 and aerosols precursors (e.g., volcanoes, ocean, soil and lightning) are kept constant at year 2000 levels; potential climate feedbacks on these sources is expected to have a small impact on surface O_3 and $PM_{2.5}$ over the United States.

In addition to climate forcing and emission changes, we include changes in land use induced by human activities in our simulations (Hurtt et al., 2011). We show projected 2050–2000 changes in crops, grasslands and trees over the US for the RCP4.5 and RCP8.5 scenarios in Fig. 1 as an example. The RCP4.5 scenario predicts an expansion of forested area, in particular over the eastern US (10 %) as a result of mitigation strategies for carbon emission reductions and a decline in agricultural land (8 %) due to this afforestation. Conversely, the RCP8.5 scenario predicts an important increase in agricultural land resulting from increasing population (up to 5 % in eastern US) and grasslands (∼ 10 %) and a decline in forest cover (2 %).

For this study, we perform nine simulations: one simulation for present-day and four for each future scenario (Table 3). For the four simulations in the future, we modify one forcing at a time, and name these simulations after their future conditions, i.e., climate alone ("2050 Climate"), anthropogenic emissions including biomass burning emissions ("2050 Emissions") and land cover and land use changes including climate-driven biogenic emissions ("2050 Land Use"). Each model simulation is initialized with a 1 year spin-up run. Following initialization, present-day and future "snapshot" forcing simulations are run for 9 years. We then average the results, and use all years to evaluate interannual variability and ultimately define statistical significance. We replicate these simulations for the RCP4.5 and RCP8.5 scenarios.

2.2 Model evaluation

The CESM simulations driven by online and offline meteorology have been extensively evaluated by comparison with satellite, sonde, aircraft and ground observations of key pollutants on a global scale (Lamarque et al., 2012). Here we focus our evaluation on annual $PM_{2.5}$ and O_3 over the United States and use long-term means from the In-

ACPD
14, 26495–26543, 2014

teragency Monitoring of Protected Visual Environments (IMPROVE) and the Clean Air Status and Trends Network (CASTNet) datasets. Both networks monitor air quality in rural areas at the surface. Figure 2 compares observed and simulated surface O_3 and $PM_{2.5}$. For O_3, we use the metric for the US EPA air quality standard of daily maximum 8 h average (MDA-8); for $PM_{2.5}$, we focus on the annual average and determine $PM_{2.5}$ fine mass as the sum of SO_4, NH_4NO_3, organic aerosol (OA), BC, fine dust and seasalt. We compute OA assuming an average molecular weight of 2.0 per carbon weight for organic carbon (Malm and Hand, 2007). Organic carbon includes SOA. We summarize the comparison between the model and observations using the squared-correlation coefficient (r^2) and the normalized mean bias (NMB) (Fig. 2c and d). In Fig. 2c, we divide the O_3 comparison into eastern and western US because of the different chemical regimes (e.g. Murazaki and Hess, 2006; Lamarque et al., 2012). For O_3, we find that simulated surface concentrations show good agreement with the mean observations over the western US (r^2 = 0.77; NMB = 4 %), whereas slightly overestimates O_3 (r^2 = 0.47; NMB = 16 %) over the eastern United States. This annual overestimation is due to a positive bias in summertime O_3 (about 10 ppb), which is a well-known issue and has been previously documented in CESM (Lamarque et al., 2012) as well as other global and regional models (e.g. Murazaki and Hess, 2006; Fiore et al., 2009; Lapina et al., 2014). Using the optimized dry deposition scheme (Sect. 2.1), we significantly improve the simulation of summertime surface O_3, which has a 30 ppb bias (NMB = 60 %) over eastern US in the standard dry deposition scheme (Val Martin et al., 2014).

For $PM_{2.5}$, we find that annual levels are well represented by CESM (r^2 = 0.70 and NMB = 12 %; Fig. 2d). We further compare the simulated $PM_{2.5}$ chemical species with observations in Fig. 3. In our simulations, SO_4 and NH_4NO_3 are somewhat overestimated, whereas OA is underestimated. BC, dust and seasalt concentrations show good agreement with the mean observations, although with some scatter in the relationship (r^2 < 0.40; not shown). These results are consistent with previous comparisons over the US (Lamarque et al., 2012; Albani et al., 2014).

ACPD
14, 26495–26543, 2014

It is important to note that in our analysis we mainly concentrate in differences between present-day and future simulations, minimizing the impact of model biases.

2.3 Studied locations

We focus our analysis in the National Parks and wilderness areas located in the continental United States as shown in Fig. 4. We consider the 352 units designated by the US National Park System in the lower 48 states, in which 46 are classified as protected parks and the rest as monuments, reserves, historical parks and sites and recreational areas. Additionally, we include 109 Class I Mandatory Federal sites that are not classified as National Park units, but in which air quality is also given special protection. In this work, we present results clustering the NPs and wilderness areas in six climatic regions (i.e., Northeast, Southeast, Midsouth, Southwest, West and Great Plains) (Hand et al., 2012). We define these regions and highlight the protected parks in Fig. 4.

3 Future changes in meteorological and chemical drivers

Climate and land cover and land use changes affect air pollution through changes in chemistry, transport, removal and natural emissions (e.g. Heald et al., 2008; Tai et al., 2012; Fiore et al., 2012). We examine here how some meteorological and chemical drivers are predicted to change in the future. Figure 5 shows present-day conditions and 2050–2000 changes in surface temperature, precipitation, boundary layer (BL) depth, isoprene emissions and O_3 dry deposition velocity. We only show changes predicted by the RCP4.5 scenario since the RCP4.5 and RCP8.5 scenarios have similar climates, but the RCP4.5 scenario has a more pronounced increase in isoprene emissions due to land use and climate change. Ozone deposition velocities also differ between the RCP4.5 and RCP8.5 simulations due to differences in projected land use change (Fig. 1). To evaluate the statistical significance of our results, we use the Student *t* test for a 95 % confidence level and highlight the regions which are signif-

ACPD
14, 26495–26543, 2014

icant. Previous studies have investigated in detail the sensitivity of surface O_3 (e.g. Murazaki and Hess, 2006; Leung and Gustafson, 2005) and $PM_{2.5}$ (e.g. Tai et al., 2012; Leibensperger et al., 2012) to numerous climatic variables. In this work, we do not intend to assess the impact that each climatic variable has on the total change in $PM_{2.5}$ and surface O_3. Instead, we provide here an overview on how these drivers may impact our simulated O_3 and $PM_{2.5}$.

Surface temperature is predicted to increase with an average of 1.7 °C across the US due to the rising greenhouse gases in the RCP 4.5 scenario (Fig. 5a). The extent of this increase varies across the US, with the maximum increase of 4 °C observed over the central United States. The RCP8.5 scenario predicts a similar increase than the RCP4.5 scenario: 2.0 °C. We find that the 9 year simulations generate robust increases in surface temperature changes across most of the continental United States. Previous studies have reported similar results with distributions and magnitudes differing slightly depending on the model, resolution and the climate scenario considered (e.g. Murazaki and Hess, 2006; Kelly et al., 2012; Pfister et al., 2014). It is known that high ozone levels correlate well with temperature in many polluted regions due to the connection between temperature to stagnation conditions, enhanced photochemistry and biogenic and wildfire emissions (Fiore et al., 2012, and references therein). $PM_{2.5}$ is also affected by many of the same meteorological processes as surface O_3, although the relationship is more complex and the sign of the effect can be positive or negative because of the different sensitivities of the $PM_{2.5}$ chemical species (e.g. Tai et al., 2012). Thus, our simulated increase in temperature will intensify surface O_3 and most probably $PM_{2.5}$ pollution over the United States.

Air quality is also sensitive to precipitation and cloud cover. For example, $PM_{2.5}$ is expected to decrease in regions with increased precipitation (e.g. Pye et al., 2009; Racherla and Adams, 2008). In our simulations, precipitation decreases over most of the continental US (30 %), with some small increases over some regions in the northwestern US (8 %) (Fig. 5b). However, not all of the changes in precipitation are significant and the absolute changes are generally small ($< 1\,mm\,day^{-1}$) despite the large

ACPD
14, 26495–26543, 2014

percentage change. We find similar pattern in the cloud cover (not shown). A decrease in cloudiness is associated with an increase in solar radiation, which favors surface O_3 production in our simulations.

An important meteorological process for diluting and transporting air pollutant is mixing within the boundary layer. In our simulations, the boundary layer depth across the US is predicted to generally increase, with the largest increase over in central US (> 100 m) (Fig. 5c). Increases in BL depth favors ventilation and reduces pollutant accumulation. In our simulations, we notice that BL depth increases (i.e., favoring low $PM_{2.5}$ and O_3 concentrations) and precipitation (and cloud cover) decreases (i.e., favoring high $PM_{2.5}$ and O_3 concentrations) are generally co-located. These two processes have opposite effects on air quality and this highlights the difficulty of predicting possible air quality impact resulting from climate change.

Higher temperature and solar radiation will also affect biogenic emissions, which in turn will influence $PM_{2.5}$ and surface O_3. Biogenic emissions will also depend on land use changes. In 2050, isoprene emissions are predicted to increase from 28 to 43 Tg C in the US (Table 2), with 10 % of this increase driven by land use changes. This effect is more significant in the southeastern US (about 25 %) due to afforestation (Fig. 5d). The RCP8.5 scenario also predicts an increase in biogenic emissions, but with a lower influence from land use and climate changes (2 %; not shown). We note that our isoprene emissions are slightly overestimated because they do not include the effect of CO_2, which suppresses isoprene production at elevated levels (e.g. Heald et al., 2008). The impact of changing biogenic emissions on surface O_3 depends critically on the fate of isoprene nitrates, i.e., whether isoprene nitrate is a terminal or temporal sink of NO_x (e.g. Horowitz et al., 2007; Wu et al., 2012). In our model, isoprene nitrate recycles 40 % of NO_x (Horowitz et al., 2007). Therefore, increases in biogenic emissions tend to enhance surface O_3. In addition, increased biogenic volatile organic compounds (e.g. isoprene) will lead to increases in $PM_{2.5}$ through SOA formation (Heald et al., 2008).

Land use changes can also influence deposition processes. For example, large O_3 dry deposition velocities are associated with denser, broadleaf forests (i.e., with high

ACPD
14, 26495–26543, 2014

LAI) and crops (e.g. Wesely, 1989; Val Martin et al., 2014), whereas grasslands and needleleaf forests (i.e., with low LAI) are characterized by low deposition velocities. In our simulations, the O_3 dry deposition velocity shows a general small decrease across the US (0.2–1.0 cm min^{-1}; about 1–3 %) (Fig. 5e). The RCP8.5 scenarios projects more variable, but even smaller changes in the O_3 dry deposition velocity (< 0.6 %), associated with a less pronounced change in vegetation. Interesting, in this study we find a reduction in the annual O_3 dry deposition velocity due to the shift from croplands to grasslands and forests. This result contrasts with previous studies that report decreased dry deposition velocities in regions with increased agricultural land (Ganzeveld et al., 2010; Wu et al., 2012). However, these studies focus on either summertime changes when the broadleaf forests have a larger dry deposition velocity than crops (Wu et al., 2012) or use a different dry deposition parameterization (Ganzeveld et al., 2010), and this underlines the important effect that land-use change assumptions have on the projections of future air quality. We note that the resulting changes in the deposition velocities in our model are not significant at the 95 % confidence level.

4 Future $PM_{2.5}$ air quality

In this section, we first examine how $PM_{2.5}$ and $PM_{2.5}$ chemical species concentrations are predicted to change in the future due to climate, emissions and land use changes. We then discuss the impacts of future climate-driven wildfire activity in $PM_{2.5}$ and haze.

4.1 Regional annual changes in $PM_{2.5}$

Figure 6 shows changes in annual surface $PM_{2.5}$ concentrations following the RCP4.5 and RCP8.5 scenarios over the continental United States. The projected changes in 2050 from the combined effects and the individual effects of emissions, climate and land use change are also shown. The "emissions" simulation takes into account changes in anthropogenic and biomass burning emissions and the "land use" simula-

ACPD
14, 26495–26543, 2014

tion is associated with changes in climate-driven biogenic emissions and land cover. We also indicate the regions with confidence levels higher than 95 % from the Student *t* test; we find that the 9 year simulations generate robust results across most of the continental US for the simulations with the combined effects and emissions alone.

The combined effects of changing climate, land use, and emissions lead to a strong decrease in $PM_{2.5}$ concentrations across the continental US (Fig. 6a), with an average projected decrease of about 4 $\mu g\,m^{-3}$ (~ 50 %) for both the RCP4.5 and RCP8.5 scenarios. The absolute decrease is stronger in the eastern than in the western US, about 4 $\mu g\,m^{-3}$ vs. 2 $\mu g\,m^{-3}$, because the eastern US is characterized by larger $PM_{2.5}$ concentrations (Fig. 2b). Projected changes in US $PM_{2.5}$ for 2050 largely reflect changes in anthropogenic emissions, which drive the majority (> 95 %) of this decrease all over the United States. The contribution of climate and land use changes, although minor and rather insignificant in most of the US, may counteract the benefits of emissions reductions in some regions (Fig. 6b). For example, the RCP4.5 scenario projects about 47 % total average decrease in $PM_{2.5}$ in the Southwest region, with about 52 % drop due to emission reductions, but a counter veiling increase of 5 and 0.1 % from climate and land use, respectively. In many regions the impact of climate and land use change is not significant compared to climate variability when averaging over 9 years.

To examine in more detail future changes in $PM_{2.5}$ we show changes in the individual $PM_{2.5}$ chemical species in Fig. 7. We find that the decrease in $PM_{2.5}$ concentrations is mainly driven by decreases in SO_4 and, to a lesser extent, in NH_4NO_3 and BC. Under the RCP4.5 and RCP8.5 scenarios, anthropogenic SO_2 emissions are projected to decrease substantially in the western and the eastern US compared to present-day (84 and 89 % in RCP4.5 and 69 and 90 % in RCP8.5, respectively; Table 2). Large decreases in NO_x emissions are also projected (75 and 78 % in RCP4.5 and 50 and 72 % in RCP8.5), whereas NH_3 emissions increase (33 and 25 % in RCP4.5 and 59 and 44 % in RCP8.5). The largest significant change in $PM_{2.5}$ is projected with the RCP8.5 scenario over the Northeast region, with a decrease of 90 % in BC, 79 % in SO_4 and 46 % in NH_4NO_3. Organic aerosol increases slightly, in particular over the

ACPD
14, 26495–26543, 2014

Northeast, Southeast and West regions. This increase does not offset the decreases in the other species, yet it can be important in some regions. Over the Southeast, the RCP4.5 and RCP8.5 scenarios project similar decreases in SO_4, NH_4NO_3 and BC. However, $PM_{2.5}$ concentrations are predicted to be lower in the RCP8.5 than in the RCP4.5 scenario because of the relative importance of OA in the total $PM_{2.5}$ loading. Higher OA concentrations in the RCP4.5 scenarios result from higher VOC emissions (Table 2) associated with reforestation and climate change, as discussed in Sect. 3.

Our results are consistent with previous studies, which have shown the small impact of climate change on $PM_{2.5}$ levels and the significant contribution from projected emissions reductions (e.g. Tagaris et al., 2007; Pye et al., 2009; Lam et al., 2011; Kelly et al., 2012). Comparing $PM_{2.5}$ projections from different studies is not straightforward due to variations in the study region, reported $PM_{2.5}$ metrics and use of different climate and emissions (Fiore et al., 2012). A decrease of about 2 $\mu g\,m^{-3}$ (25 %) over the US was projected for the SRES A1B scenario by Tagaris et al. (2007) for the combined effect of climate and emissions, with the bulk of this decrease resulting from sulfate, nitrate and ammonium reductions. Using the same scenario, Lam et al. (2011) found a similar decrease (4–5 $\mu g\,m^{-3}$), with 90 % of the reduction due to emission reductions. Most recently, Kelly et al. (2012) reported summertime regional decreases of more than 3 $\mu g\,m^{-3}$ over the US, with the SRES A2 climate and RCP6.0 emission scenarios.

We summarize the simulated $PM_{2.5}$ changes over the US NP and wilderness areas in Table 4. We show results for the 46 protected National Parks located in the continental United States. We find that the RCP4.5 and RCP8.5 scenarios predict a significant reduction of $PM_{2.5}$ levels across the protected NPs, with the exception of the Crater Lake and Lassen Volcanic NPs. In these two NPs, the RCP8.5 scenario projects a slight increase in annual $PM_{2.5}$, but concentrations are predicted to remain below 12 $\mu g\,m^{-3}$, the primary annual US National Ambient Air Quality Standards (NAAQS) for $PM_{2.5}$. In the Joshua Tree NP, both RCP scenarios predict a significant improvement of $PM_{2.5}$ air quality, but with an annual average above 12 $\mu g\,m^{-3}$ due to the dominance of natural dust in this region.

ACPD
14, 26495–26543, 2014

It is important to note that changes in the frequency and magnitude of the fire resulting from climate change are not included in this analysis, and this effect may have an important impact on the $PM_{2.5}$ levels associated with climate change, as discussed in the following section.

4.2 Effects of increased fire activity on summertime $PM_{2.5}$

Climate-driven changes in fire emissions can be an important factor controlling $PM_{2.5}$ concentrations (Spracklen et al., 2009; Yue et al., 2013). Yue et al. (2013), use results from 15 climate models following the SRES A1B scenario and a fire prediction model of area burned to predict increases of 63–169 % in area burned over the western US in 2050, which leads to about 150–170 % increases in OC and BC fire emissions. The RCP4.5 scenario predicts an increase of about 60 % in OC fire emissions over the western US, whereas the RCP8.5 projects a marginal decrease of 0.3 %. These two RCP scenarios clearly underestimate the average increase in carbonaceous aerosol fire emissions associated with climate feedbacks as projected by Yue et al. (2013).

To assess the importance of climate-driven fire emissions on future $PM_{2.5}$, we perform an additional simulation (not shown in Table 3), where we increase the RCP fire emissions over the US in order to match Yue et al. (2013)'s projection. In doing so, we keep the spatial distribution of fire as described by the RCP scenarios and apply a homogeneous increase on a monthly basis. We scale the RCP fire emissions over the US and Canada, with the exception of the eastern US, where fire activity is not predicted to significantly increase in the future due to climate (Scholze et al., 2006; Moritz et al., 2012).

Figure 8 shows the effect of climate-driven fire emissions on summertime $PM_{2.5}$. We focus on the summer here which is the peak fire season in the United States. We compare the $PM_{2.5}$ levels predicted by the RCP scenarios in 2050 to those when climate-driven fire activity is included, and only show those climatic regions where $PM_{2.5}$ is affected by fire, i.e., West, Great Plains, Southwest and Northeast. $PM_{2.5}$ concentrations in these regions increase significantly as a result of increased fire activity. These

ACPD
14, 26495–26543, 2014

increases are most prominent over the West and Great Plain regions, in which fire-driven $PM_{2.5}$ may potentially offset anticipated reductions in anthropogenic emissions. For example, over the West region we estimate that fire activity may increase future summertime $PM_{2.5}$ from 3.2 to 5.2 $\mu g\,m^{-3}$ (63 %) in the RCP8.5 scenario and from 4.5 to 5.6 $\mu g\,m^{-3}$ (22 %) in the RCP4.5 scenario. The concentration of organic aerosol nearly doubles in both scenarios, and this dominates the total change in $PM_{2.5}$. It is important to note that our fire OA may be underestimated as we do not include secondary production of OA from fire emissions. Increased fire activity may also affect $PM_{2.5}$ further downwind from the fires. We estimate that summertime $PM_{2.5}$ may increase up to 4–10 % in the Northeast region due to smoke transported from fires in the western US and the boreal region.

Therefore, changes in summertime $PM_{2.5}$ concentrations may be dominated by changes in fire activity in most of the western US in a future climate. This same fire pollution may contribute significantly to impairing visibility over this region, as well as hundreds of kilometers downwind from the fire sources.

4.3 Effects on future visibility

We evaluate the effects of future changes in visibility in the US NP and wilderness areas across the continental US by examining changes in the haze index (HI) and visibility range. We calculate the HI based on the definition of the US EPA (2003) and the visibility range as in Pitchford and Malm (1994) using the results of the daily averages of $PM_{2.5}$ chemical species. Figure 9a shows changes in HI for the most polluted and the cleanest episodes predicted by the RCP4.5 and RCP8.5 scenarios. We define most polluted and cleanest episodes as those days characterized by aerosol levels with the 20 % worst and best visibility, that is, with the HI above the 90th percentile or below the 10th percentile, respectively (US EPA, 2003). As an example, we show in Fig. 9b the cumulative distribution function of daily HI over two protected national parks: Crater Lake and Acadia NP, located over the West and Northeast region, respectively. We also include the impact of fire pollution in this analysis and indicate the 2050 HI target

ACPD
14, 26495–26543, 2014

required to reach natural background conditions by 2064 as mandated by the Regional Haze Rule.

Consistent with the $PM_{2.5}$ projections, we predict a significant visibility improvement in both polluted and background conditions over the continental United States. This improvement results mainly from the large reduction in anthropogenic emissions, with the strongest absolute reductions in areas with high $PM_{2.5}$ and high anthropogenic aerosol precursor emissions such as the Northeast region. In this region, our results show a reduction of up to 15 deciviews during cleanest days and up to 10 deciviews during most polluted events in both RCP scenarios, which corresponds to an increase of more than 75 km in visibility range.

The improvement in $PM_{2.5}$ air quality is reflected in the projected visibility over the US National Parks and wilderness areas. For example, in Acadia NP, we find that both RCP scenarios predict HI level decreases of about 10 deciviews during the most polluted events, leading to an improvement in visibility range of more than 70 km. This NP is estimated to reach the 2050 target to restore natural visibility conditions by 2064, even during most polluted conditions. However, this is not the case for all the protected NPs and wilderness areas. Our results show that visibility in Crater Lake NP is estimated to improve by 2050, with moderate HI decreases ($\sim$ 4 deciviews) predicted by both RCP scenarios, and a general improvement of visibility range of 30–40 km. However, HI levels are predicted to remain higher than the 2050 target. This is also the case for other important NPs located in the western US such as Yellowstone, Grand Canyon, and Mount Rainier NPs; about 40 and 74 % of the total parks may not reach the 2050 target as predicted by the RCP4.5 and RCP8.5 scenarios, respectively.

Future regional visibility may also be impaired by fire pollution resulting from climate change. We find that fire pollution may maintain visibility levels at present-day conditions during the most polluted events in some NPs and wilderness areas (e.g. Crater Lake NP; Fig. 9b) or may impede the attainment of the 2050 visibility target (e.g. Yellowstone NP; not shown). Our analysis shows little or no effect of fire in visibility impairment in NPs and wilderness areas located in the Northeast and Southeast climatic

ACPD
14, 26495–26543, 2014

regions (e.g., Acadia NP; Fig. 9b). Yue et al. (2013) estimate that future fire activity would lead to an average visibility decrease of 30 km in the 32 Federal Class I areas located in Rocky Mountains Forest. Our predictions for the Rocky Mountain NP show more moderate decreases in visibility (4–6 km; not shown). However, our work differs from Yue et al. (2013) in both the model resolution (200 vs. 400 km) and the spatial distribution of the fire emissions.

5 Future changes in surface O_3

In this section, we first examine future projections on daily surface O_3 concentrations and evaluate the contributing factors to this future change. We then discuss how future changes in surface O_3 may impact ecosystems.

5.1 Predictions of daily O_3 concentrations

Figure 10 shows the 2050–2000 changes in annual mean surface O_3 concentrations predicted by the RCP4.5 and RCP8.5 scenarios in the continental United States. As in the $PM_{2.5}$ analysis, we present total changes in the simulated daily MDA-8 O_3 concentrations and show the individual perturbations resulting from changing climate, land use, and reducing emission (Fig. 10a). We also highlight the regions with confidence levels higher than 95 % from the Student *t* test.

The combined effects of changing emissions, climate and land use produce a strong decrease in surface O_3 across the continental US in the RCP4.5 scenario, with the strongest absolute reductions (up to 10 ppb) over the eastern US and California, regions with the highest O_3 concentrations (Fig. 2a) and strongest anthropogenic precursors emissions reductions. The average MDA-8 over the US decreases from 52 to 47 ppb from present to future days. However, the RCP8.5 scenario predicts important increases over the Great Plain region (about 5 ppb) and marginal decreases (about 1 ppb) over the eastern US and California. The RCP4.5 and RCP8.5 scenarios project

ACPD
14, 26495–26543, 2014

strong and similar decreases in domestic O_3 precursor emissions (Table 2), however global CH_4 concentrations are 50 % larger in RCP8.5 compared to RCP4.5 (2740 vs. 1838 ppb; Table 1). Rising surface O_3 levels over central US are therefore the result of elevated background O_3 due to rising CH_4 levels in combination with climate and land use changes. These individual effects can be clearly seen in Fig. 10b, which shows that climate and land use changes completely offset the emission reductions over the West and Midsouth regions in the RCP8.5 scenario. For example, in the West region, the RCP8.5 scenario predicts an overall increase of 3 % in surface O_3 ($\sim$ 3 ppb), in which the contribution from emission reductions (−2 %) is counterbalance by climate (+3 %) and land (+2 %) changes.

The impact of the rising background O_3 in the RCP8.5 scenario can also be seen on the surface O_3 concentrations over the ocean. Similar to previous studies (e.g. Wu et al., 2008; Fiore et al., 2012), the RCP4.5 scenario projects a decrease in O_3 levels (up to 5 ppb) over the Pacific and Atlantic oceans in a changing climate due to the decrease of O_3 lifetime associated with higher water vapor. The shorter lifetime of PAN in a future climate may also contribute to the decrease of O_3 levels over remote areas (e.g. Wu et al., 2008; Doherty et al., 2013). By contrast, the RCP8.5 scenario projects an increase in surface O_3 (up to 8 ppb) due to the rising background over these remote regions.

Climate and land use changes alone are also expected to significantly impact future O_3 air quality. When only climate change is considered and the emissions of ozone precursors are held at present-day levels ("Climate" simulation), simulated surface O_3 increases by 1 and 2 ppb across the US in the RCP4.5 and RCP8.5 scenarios respectively, with the largest absolute changes over the eastern US (up to 3 and 5 ppb, respectively). Note that this "climate penalty" does not include the effect of changing biogenic emissions, which is incorporated in the land use change simulations. However, Tai et al. (2013) show that the offsetting effects of climate and CO_2 inhibition substantially reduce the role of isoprene emission changes in the climate penalty. Thus, the climate effect shown here may be a good proxy for the climate penalty and is compara-

ACPD
14, 26495–26543, 2014

ble to values shown by Tai et al. (2013). In the land use change simulation, surface O_3 increases by 2 ppb in both scenarios, with the largest increases over the central US (up to 8 and 4 ppb, respectively). Increases in surface O_3 result mainly from climate-driven increases in biogenic VOCs and, to a lesser extent, from a decrease in dry deposition velocity due to the shift from croplands to grasslands projected in both scenarios over this region. We also note that our land use impacts are slightly overestimated because we do not include the effect of CO_2 inhibition in our isoprene emissions, as discussed in Sect. 3.

Our projected change in surface O_3 is more moderate than that reported in previous studies (e.g. Tagaris et al., 2007; Nolte et al., 2008; Kelly et al., 2012; Pfister et al., 2014). However, these studies do not account for changes in land cover, which our work indicates can be regionally quite substantial.

Figure 11 shows the impact of these changes on surface O_3 over the US National Parks and wilderness areas. Under RCP8.5 conditions, we find an improvement of surface O_3 air quality for most polluted days (i.e. high tail of the distribution is lower than present-day), except in the Great Plains region, and a deterioration in the background O_3 (i.e., the low tail of the distribution is higher than present-day) all across the United States. These results are due to increases in CH_4 emissions in combination with the effects of climate and land use changes as discussed above. However, under RCP4.5 conditions, there is a clear general improvement of surface O_3 air quality across the US, with the exception of increasing background O_3 in the Northeast, Southeast and Midsouth regions. Furthermore, as discussed in Pfister et al. (2014), background O_3 at high elevations may be affected by long-range transport of pollution and stratospheric intrusions (e.g. Eyring et al., 2010; Lin et al., 2012). Both processes are taken into account in our simulations (but not disaggregated), and are expected to change in the future due to decreasing NO_x emissions in Asia (van Vuuren et al., 2011) and the recovery of the stratosphere O_3 layer (Eyring et al., 2010; Kawase et al., 2011).

In all of the US protected NPs and wilderness areas (Table 4), surface O_3 levels are predicted to improve under the RCP4.5 scenario. We estimate that annual concentra-

ACPD
14, 26495–26543, 2014

tions are projected to be below the current primary EPA NAAQS of 75 ppb to protect public health, and even below a more restrictive potential future standard of 65 ppb. In contrast, under RCP8.5 conditions, numerous parks and wilderness areas are predicted to have poorer O_3 air quality. For example, 34 out of the 46 protected NPs in the lower 48 states may encounter surface O_3 increases with respect to present-day levels (e.g., Glacier and Yellowstone NPs), although projected concentrations are below 65 ppb. However, during the summer, when O_3 concentrations are higher, 16 out of 46 NPs are predicted to have summertime surface O_3 levels above 65 ppb (e.g., Rocky Mountain and Yosemite NPs) (not shown).

5.2 Effects on future ecosystem O_3 damage

To investigate the effect of projected changes in surface O_3 levels in the US NPs and wilderness areas, we use the secondary metric W126 established to protect ecosystems and crops. The W126 is a biologically based index that estimates a cumulative ozone exposure over a 3 month growing season and applies sigmoidal weighting to hourly ozone concentrations (e.g. Lefohn et al., 1988; Lapina et al., 2014). Figure 12 presents average W126 over the US NPs and wilderness areas divided in the 6 climatic regions for present-day and future. We focus on summertime W126 as the summer season is the growing season for many ecosystems. The spatial distribution of W126 (not shown) is similar to the MDA-8 O_3 (Fig. 2a), but with the regions of low and high ozone more emphasized due to the sigmoidal weighting of the W126 function as discussed in Lapina et al. (2014).

Consistent with the daily O_3 pattern, the RCP4.5 and RCP8.5 scenarios project a decrease in the W126 index across the continental US, with the exception of the Great Plain region by the RCP8.5 scenario. Despite the general decrease in daily surface O_3 predicted by both scenarios from strong emission reductions, our results show that the W126 index may remain above the suggested range for a secondary standard (7–15 ppm h) throughout most of the United States. Under RCP8.5 conditions, our simulations predict that the W126 index will remain above the maximum recommended limit

ACPD
14, 26495–26543, 2014

(15 ppm h) to protect vegetation, with the exception of the Southeast region, where W126 will still remain above the minimum recommended limit (7 ppm h). The RCP4.5 scenario predicts lower W126 levels, yet still above the minimum recommended standard in almost all the regions.

The simulated W126 over the US protected NPs is summarized in Table 4. Our study shows that a number of protected NPs will experience W126 levels exceeding the secondary standard to protect vegetation. The RCP8.5 scenarios projects that the majority of the protected parks will have an W126 index above the recommended limits, with 34 parks above 7 ppm h and 26 parks above 15 ppm h; projections from the RCP4.5 result in 26 and 6 parks, respectively. Therefore, O_3 pollution may remain a threat to ecosystems in the US NPs and wilderness areas despite the substantial general decrease in surface O_3 concentrations.

6 Conclusions

We have quantified for the first time changes in air quality between present and a 2050 future period associated with changes in emissions, climate, and land use change over the United States. In particular, we focus on the implications of these projections for air quality in National Parks and wilderness areas.

We find that, if stringent domestic emission controls are applied in the future such as those projected by the RCP4.5 and RCP8.5 scenarios, air quality is predicted to improve significantly across the US, except surface O_3 in the central US under RCP8.5 conditions. We estimate that $PM_{2.5}$ concentrations in the majority of the US NPs and wilderness areas will be substantially reduced, below the annual US EPA NAAQS of 12 $\mu g\,m^{-3}$. In addition, visibility will be in general significantly improved. Over the eastern US, we estimate that most of the parks will reach the 2050 target to restore visibility to natural conditions by 2064, whereas some parks may not reach this target during most polluted episodes over the western US (e.g., Yellowstone and Grand Canyon NP). This result suggests that, to obtain acceptable future visibility conditions over this

ACPD
14, 26495–26543, 2014

region, the US National Park Service may have to develop specific air quality management plans to include further mitigation strategies beyond those projected by the RCP scenarios.

Our analysis shows that climate-driven fires may dominate summertime $PM_{2.5}$ concentrations in the future over the western US, potentially offsetting the large $PM_{2.5}$ reductions from anthropogenic emission controls. Future regional visibility is also estimated to be impaired by fire pollution, which may keep visibility at present-day levels during the most polluted episodes in many parks (e.g., Crater Lake NP). However, our analysis has important limitations. For example, it considers an average fire emission projection based on SRES A1B climate and applies this projection homogeneously to all the fire species on a monthly basis and with the spatial distribution formulated by the RCP fire emission database. More work is needed to directly couple climate-driven fire emissions, vegetation dynamics, and air quality.

We find that daily surface O_3 is projected to drop in all US NPs and wilderness areas in the RCP4.5 scenario, with MDA-8 levels below the primary US EPA NAAQS of 75 ppb to protect human health, and even below 65 ppb, a level considered for future regulation. In contrast, our projections with the RCP8.5 scenario indicate that numerous parks in the western and central US are predicted to have a poorer O_3 air quality, with MDA-8 above 65 ppb in some cases during the summer (e.g., Rocky Mountain and Yellowstone NP). In this case, the rising O_3 resulting from a growing O_3 background associated with increases in CH_4 levels ($\sim$ 1000 ppb) as well as climate and land use changes exceeds the important surface O_3 reductions projected from anthropogenic emission controls. Furthermore, despite the substantial general decrease in surface O_3, our study indicates that the secondary standard W126 may remain above the recommended limits (7–15 ppm h) to protect vegetation in many regions across the United States. Thus, future O_3 pollution may be a threat to the US NP ecosystems. In the US, W126 levels are most sensitive to domestic anthropogenic NO_x emissions (Lapina et al., 2014) and our results suggest that more restricted policies for NO_x control may be needed to preserve natural ecosystems in the US NPs and wilderness areas.

ACPD
14, 26495–26543, 2014

Our results suggest that 2050 air quality in the US will likely be dominated by anthropogenic emission trajectories. Changes in air quality driven by climate and land use are small over the 50 year time horizon studied and they are not always significant. However, climate alone can lead to a substantial increase in surface MDA-8 O_3 by 2050 over most of the US with important implications for O_3 air quality and ecosystem health degradation at the US National Parks. Projected changes in temperature, cloud cover, and biogenic emissions suggest that these drivers may exacerbate future O_3 pollution across the United States. Furthermore, land use change may have an important regional effect on surface O_3, due to changes in biogenic emissions and dry deposition. Our study suggests that the effects of climate, vegetation, and fires are important in future air quality projections and these processes should be considered in air quality management and planning in the coming decades.

Acknowledgements. This work was supported by the US National Park Service (grant H2370 094000/J2350103006), the US National Science Foundation (AGS-1238109), and the JFSP (project ID 13-1-01-4). We thank Xu Yue (Yale University) and Jenny Hand (CIRAS-CSU) for helpful discussions and Samuel Albani (Cornell University) for the updated dust scheme. The CESM project is supported by the National Science Foundation and the Office of Science (BER) of the US Department of Energy. Computing resources were provided by the Climate Simulation Laboratory at NCAR's Computational and Information Systems Laboratory (CISL), sponsored by the National Science Foundation and other agencies. The National Center for Atmospheric Research is operated by the University Corporation for Atmospheric Research under sponsorship of the National Science Foundation. Any opinions, findings, and conclusions or recommendations expressed in this material are those of the author(s) and do not necessarily reflect the views of the National Science Foundation.

References

Albani, S., Mahowald, N. M., Perry, A. T., Scanza, R. A., Heavens, N. G., Zender, C. S., Maggi, V., Kok, J. F., and Otto-Bliesner, B. L.: Improved dust representation in the Commu-

ACPD
14, 26495–26543, 2014

nity Atmosphere Model, J. Adv. Model. Earth Syst., 6, doi:10.1002/2013MS000279, 2014. 26500, 26501, 26503

Arbaugh, M. J., Miller, P. R., Carroll, J. J., Takemoto, B., and Procter, T.: Relationships of ozone exposure to pine injury in the Sierra Nevada and San Bernardino Mountains of California, USA, Environ. Pollut., 101, 291–301, doi:10.1016/S0269-7491(98)00027-X, 1998. 26498

Arneth, A., Harrison, S. P., Zaehle, S., Tsigaridis, K., Menon, S., Bartlein, P. J., Feichter, J., Korhola, A., Kulmala, M., O'Donnell, D., Schurgers, G., Sorvari, S., and Vesala, T.: Terrestrial biogeochemical feedbacks in the climate system, Nat. Geosci., 3, 525–532, doi:10.1038/ngeo905, 2010. 26497

Avnery, S., Mauzerall, D. L., Liu, J., and Horowitz, L. W.: Global crop yield reductions due to surface ozone exposure: 1. Year 2000 crop production losses and economic damage, Atmos. Environ., 45, 2284–2296, doi:10.1016/j.atmosenv.2010.11.045, 2011. 26498

Doherty, R. M., Wild, O., Shindell, D. T., Zeng, G., MacKenzie, I. A., Collins, W. J., Fiore, A. M., Stevenson, D. S., Dentener, F. J., Schultz, M. G., Hess, P., Derwent, R. G., and Keating, T. J.: Impacts of climate change on surface ozone and intercontinental ozone pollution: a multi-model study, J. Geophys. Res.-Atmos., 118, 3744–3763, doi:10.1002/jgrd.50266, 2013. 26514

Emmons, L. K., Walters, S., Hess, P. G., Lamarque, J.-F., Pfister, G. G., Fillmore, D., Granier, C., Guenther, A., Kinnison, D., Laepple, T., Orlando, J., Tie, X., Tyndall, G., Wiedinmyer, C., Baughcum, S. L., and Kloster, S.: Description and evaluation of the Model for Ozone and Related chemical Tracers, version 4 (MOZART-4), Geosci. Model Dev., 3, 43–67, doi:10.5194/gmd-3-43-2010, 2010. 26500

Eyring, V., Cionni, I., Bodeker, G. E., Charlton-Perez, A. J., Kinnison, D. E., Scinocca, J. F., Waugh, D. W., Akiyoshi, H., Bekki, S., Chipperfield, M. P., Dameris, M., Dhomse, S., Frith, S. M., Garny, H., Gettelman, A., Kubin, A., Langematz, U., Mancini, E., Marchand, M., Nakamura, T., Oman, L. D., Pawson, S., Pitari, G., Plummer, D. A., Rozanov, E., Shepherd, T. G., Shibata, K., Tian, W., Braesicke, P., Hardiman, S. C., Lamarque, J. F., Morgenstern, O., Pyle, J. A., Smale, D., and Yamashita, Y.: Multi-model assessment of stratospheric ozone return dates and ozone recovery in CCMVal-2 models, Atmos. Chem. Phys., 10, 9451–9472, doi:10.5194/acp-10-9451-2010, 2010. 26515

Fiore, A. M., Dentener, F. J., Wild, O., Cuvelier, C., Schultz, M. G., Hess, P., Textor, C., Schulz, M., Doherty, R. M., Horowitz, L. W., MacKenzie, I. A., Sanderson, M. G., Shindell, D. T., Stevenson, D. S., Szopa, S., Van Dingenen, R., Zeng, G., Atherton, C.,

ACPD
14, 26495–26543, 2014

Bergmann, D., Bey, I., Carmichael, G., Collins, W. J., Duncan, B. N., Faluvegi, G., Folberth, G., Gauss, M., Gong, S., Hauglustaine, D., Holloway, T., Isaksen, I. S. A., Jacob, D. J., Jonson, J. E., Kaminski, J. W., Keating, T. J., Lupu, A., Marmer, E., Montanaro, V., Park, R. J., Pitari, G., Pringle, K. J., Pyle, J. A., Schroeder, S., Vivanco, M. G., Wind, P., Wojcik, G., Wu, S., and Zuber, A.: Multimodel estimates of intercontinental source-receptor relationships for ozone pollution, J. Geophys. Res., 114, D04301, doi:10.1029/2008JD010816, 2009. 26503

Fiore, A. M., Naik, V., Spracklen, D. V., Steiner, A., Unger, N., Prather, M., Bergmann, D., Cameron-Smith, P. J., Cionni, I., Collins, W. J., Dalsoren, S., Eyring, V., Folberth, G. A., Ginoux, P., Horowitz, L. W., Josse, B., Lamarque, J.-F., MacKenzie, I. A., Nagashima, T., O'Connor, F. M., Righi, M., Rumbold, S. T., Shindell, D. T., Skeie, R. B., Sudo, K., Szopa, S., Takemura, T., and Zeng, G.: Global air quality and climate, Chem. Soc. Rev., 41, 6663–6683, doi:10.1039/C2CS35095E, 2012. 26497, 26504, 26505, 26509, 26514

Ganzeveld, L., Bouwman, L., Stehfest, E., van Vuuren, D. P., Eickhout, B., and Lelieveld, J.: Impact of future land use and land cover changes on atmospheric chemistry-climate interactions, J. Geophys. Res., 115, D23301, doi:10.1029/2010JD014041, 2010. 26497, 26507

Ghude, S. D., Jena, C., Chate, D. M., Beig, G., Pfister, G. G., Kumar, R., and Ramanathan, V.: Reductions in India's crop yield due to ozone, Geophys. Res. Lett., 41, 5685–5691, doi:10.1002/2014GL060930, 2014. 26498

Guenther, A. B., Jiang, X., Heald, C. L., Sakulyanontvittaya, T., Duhl, T., Emmons, L. K., and Wang, X.: The Model of Emissions of Gases and Aerosols from Nature version 2.1 (MEGAN2.1): an extended and updated framework for modeling biogenic emissions, Geosci. Model Dev., 5, 1471–1492, doi:10.5194/gmd-5-1471-2012, 2012. 26501

Hand, J. L., Schichtel, B. A., Malm, W. C., and Pitchford, M. L.: Particulate sulfate ion concentration and SO_2 emission trends in the United States from the early 1990s through 2010, Atmos. Chem. Phys., 12, 10353–10365, doi:10.5194/acp-12-10353-2012, 2012. 26504

Heald, C. L., Henze, D. K., Horowitz, L. W., Feddema, J., Lamarque, J.-F., Guenther, A., Hess, P. G., Vitt, F., Seinfeld, J. H., Goldstein, A. H., and Fung, I.: Predicted change in global secondary organic aerosol concentrations in response to future climate, emissions, and land use change, J. Geophys. Res.-Atmos., 113, D05211, doi:10.1029/2007JD009092, 2008. 26497, 26501, 26504, 26506

Horowitz, L. W., Fiore, A. M., Milly, G. P., Cohen, R. C., Perring, A., Wooldridge, P. J., Hess, P. G., Emmons, L. K., and Lamarque, J.-F.: Observational constraints on the chemistry of iso-

ACPD
14, 26495–26543, 2014

prene nitrates over the eastern United States, J. Geophys. Res.-Atmos., 112, D12S08, doi:10.1029/2006JD007747, 2007. 26506

Hurtt, G., Chini, L., Frolking, S., Betts, R., Feddema, J., Fischer, G., Fisk, J., Hibbard, K., Houghton, R., Janetos, A., Jones, C., Kindermann, G., Kinoshita, T., Klein Goldewijk, K., Riahi, K., Shevliakova, E., Smith, S., Stehfest, E., Thomson, A., Thornton, P., Vuuren, D., and Wang, Y.: Harmonization of land-use scenarios for the period 1500–2100: 600 years of global gridded annual land-use transitions, wood harvest, and resulting secondary lands, Climatic Change, 109, 117–161, doi:10.1007/s10584-011-0153-2, 2011. 26502

IPCC: Climate Change 2013: The Physical Science Basis, edited by: Stocker, T., Qin, D., Plattner, G.-K., Tignor, M., Allen, S., Boschung, J., Nauels, A., Y. Xia, V. B., and Midgley, P., Cambridge University Press, Cambridge, UK and New York, NY, USA, 1535 pp., 2013. 26497, 26499

Jacob, D. J. and Winner, D. A.: Effect of climate change on air quality, Atmos. Environ., 43, 51–63, doi:10.1016/j.atmosenv.2008.09.051, 2009. 26497

Kawase, H., Nagashima, T., Sudo, K., and Nozawa, T.: Future changes in tropospheric ozone under Representative Concentration Pathways (RCPs), Geophys. Res. Lett., 38, L05801, doi:10.1029/2010GL046402, 2011. 26515

Kelly, J., Makar, P. A., and Plummer, D. A.: Projections of mid-century summer air-quality for North America: effects of changes in climate and precursor emissions, Atmos. Chem. Phys., 12, 5367–5390, doi:10.5194/acp-12-5367-2012, 2012. 26505, 26509, 26515

Lack, D. A., Tie, X. X., Bofinger, N. D., Wiegand, A. N., and Madronich, S.: Seasonal variability of secondary organic aerosol: a global modeling study, J. Geophys. Res.-Atmos., 109, D03203, doi:10.1029/2003JD003418, 2004. 26500

Lam, Y. F., Fu, J. S., Wu, S., and Mickley, L. J.: Impacts of future climate change and effects of biogenic emissions on surface ozone and particulate matter concentrations in the United States, Atmos. Chem. Phys., 11, 4789–4806, doi:10.5194/acp-11-4789-2011, 2011. 26509

Lamarque, J.-F., Bond, T. C., Eyring, V., Granier, C., Heil, A., Klimont, Z., Lee, D., Liousse, C., Mieville, A., Owen, B., Schultz, M. G., Shindell, D., Smith, S. J., Stehfest, E., Van Aardenne, J., Cooper, O. R., Kainuma, M., Mahowald, N., McConnell, J. R., Naik, V., Riahi, K., and van Vuuren, D. P.: Historical (1850–2000) gridded anthropogenic and biomass burning emissions of reactive gases and aerosols: methodology and application, Atmos. Chem. Phys., 10, 7017–7039, doi:10.5194/acp-10-7017-2010, 2010. 26501

ACPD
14, 26495–26543, 2014

Lamarque, J.-F., Emmons, L. K., Hess, P. G., Kinnison, D. E., Tilmes, S., Vitt, F., Heald, C. L., Holland, E. A., Lauritzen, P. H., Neu, J., Orlando, J. J., Rasch, P. J., and Tyndall, G. K.: CAM-chem: description and evaluation of interactive atmospheric chemistry in the Community Earth System Model, Geosci. Model Dev., 5, 369–411, doi:10.5194/gmd-5-369-2012, 2012. 26500, 26502, 26503

Lapina, K., Henze, D. K., Milford, J. B., Huang, M., Lin, M., Fiore, A. M., Carmichael, G., Pfister, G. G., and Bowman, K.: Assessment of source contributions to seasonal vegetative exposure to ozone in the U.S., J. Geophys. Res., 119, 324–340, doi:10.1002/2013JD020905, 2014. 26503, 26516, 26518

Lefohn, A. S., Laurence, J. A., and Kohut, R. J.: A comparison of indices that describe the relationship between exposure to ozone and reduction in the yield of agricultural crops, Atmos. Environ., 22, 1229–1240, doi:10.1016/0004-6981(88)90353-8, 1988. 26516

Leibensperger, E. M., Mickley, L. J., Jacob, D. J., Chen, W.-T., Seinfeld, J. H., Nenes, A., Adams, P. J., Streets, D. G., Kumar, N., and Rind, D.: Climatic effects of 1950–2050 changes in US anthropogenic aerosols – Part 1: Aerosol trends and radiative forcing, Atmos. Chem. Phys., 12, 3333–3348, doi:10.5194/acp-12-3333-2012, 2012. 26505

Leung, L. R. and Gustafson, W. I.: Potential regional climate change and implications to U. S. air quality, Geophys. Res. Lett., 32, L16711, doi:10.1029/2005GL022911, 2005. 26505

Lin, M., Fiore, A. M., Horowitz, L. W., Cooper, O. R., Naik, V., Holloway, J., Johnson, B. J., Middlebrook, A. M., Oltmans, S. J., Pollack, I. B., Ryerson, T. B., Warner, J. X., Wiedinmyer, C., Wilson, J., and Wyman, B.: Transport of Asian ozone pollution into surface air over the western United States in spring, J. Geophys. Res.-Atmos., 117, D00V07, doi:10.1029/2011JD016961, 2012. 26515

Mahowald, N. M., Lamarque, J.-F., Tie, X. X., and Wolff, E.: Sea-salt aerosol response to climate change: Last Glacial Maximum, preindustrial, and doubled carbon dioxide climates, J. Geophys. Res.-Atmos., 111, D05303, doi:10.1029/2005JD006459, 2006a. 26500, 26501

Mahowald, N. M., Muhs, D. R., Levis, S., Rasch, P. J., Yoshioka, M., Zender, C. S., and Luo, C.: Change in atmospheric mineral aerosols in response to climate: last glacial period, preindustrial, modern, and doubled carbon dioxide climates, J. Geophys. Res.-Atmos., 111, D10202, doi:10.1029/2005JD006653, 2006b. 26500, 26501

Malm, W. C. and Hand, J. L.: An examination of the physical and optical properties of aerosols collected in the {IMPROVE} program, Atmos. Environ., 41, 3407–3427, doi:10.1016/j.atmosenv.2006.12.012, 2007. 26503

ACPD
14, 26495–26543, 2014

Meehl, G. A., Hu, A., Tebaldi, C., Arblaster, J. M., Washington, M. W., Teng, H., Sanderson, B. M., Ault, T., Strand, W. G., and White, J. B.: Relative outcomes of climate change mitigation related to temperature versus sea level and sea level rise, Nature Climate Change, 2, 576–580, doi:10.1038/nclimate1529, 2012. 26501

Metzger, S., Dentener, F., Pandis, S., and Lelieveld, J.: Gas/aerosol partitioning: 1. A computationally efficient model, J. Geophys. Res.-Atmos., 107, ACH 16-1–ACH 16-24, doi:10.1029/2001JD001102, 2002. 26500

Moritz, M. A., Parisien, M.-A., Batllori, E., Krawchuk, M. A., Van Dorn, J., Ganz, D. J., and Hayhoe, K.: Climate change and disruptions to global fire activity, Ecosphere, 3, 49, doi:10.1890/ES11-00345.1, 2012. 26510

Moss, R. H., Edmonds, J. A., Hibbard, K. A., Manning, M. R., Rose, S. K., van Vuuren, D. P., Carter, T. R., Emori, S., Kainuma, M., Kram, T., Meehl, G. A., Mitchell, J. F. B., Nakicenovic, N., Riahi, K., Smith, S. J., Stouffer, R. J., Thomson, A. M., Weyant, J. P., and Wilbanks, T. J.: The next generation of scenarios for climate change and assessment, Nature, 463, 747–756, doi:10.1038/nature08823, 2011. 26501

Murazaki, K. and Hess, P.: How does climate change contribute to surface ozone change over the United States?, J. Geophys. Res., 111, D05301, doi:10.1029/2005JD005873, 2006. 26503, 26505

Neale, R. B., Richter, J., Park, S., Lauritzen, P. H., Vavrus, S. J., Rasch, P. J., and Zhang, M.: The mean climate of the community atmosphere model (CAM4) in forced SST and fully coupled experiments., J. Climate, 26, 5150–5168, doi:10.1175/JCLI-D-12-00236.1, 2013. 26500

Nolte, C. G., Gilliland, A. B., Hogrefe, C., and Mickley, L. J.: Linking global to regional models to assess future climate impacts on surface ozone levels in the United States, J. Geophys. Res.-Atmos., 113, D14307, doi:10.1029/2007JD008497, 2008. 26515

Oleson, K. W., Lawrence, D. M., Bonan, G. B., Flanner, M. G., Kluzek, E., Lawrence, P. J., Levis, S., Swenson, S. C., Thornton, P. E., Dai, A., M., D., Dickinson, R., Feddema, J., Heald, C. L., Hoffman, F., Lamarque, J.-F., Mahowald, N., Niu, G.-Y., Qian, T., Randerson, J., Running, S., Sakaguchi, K., Slater, A., Stockli, R., Wang, A., Yang, Z.-L., and Zeng, X.: Technical description of version 4.0 of the Community Land Model (CLM), Tech. Rep. Technical Note NCAR/TN-478+STR, 257 pp., NCAR, 2010. 26499

Pfister, G. G., Walters, S., Lamarque, J.-F., Fast, J., Barth, M. C., Wong, J., Done, J., Holland, G., and Brussere, C. L.: Projections of future summertime ozone over the U. S., J.

ACPD
14, 26495–26543, 2014

Geophys. Res.-Atmos., 119, 5559–5582, doi:10.1002/2013JD020932, 2014. 26497, 26505, 26515
Pitchford, M. L. and Malm, W. C.: Development and applications of a standard visual index, Atmos. Environ., 28, 1049–1054, doi:10.1016/1352-2310(94)90264-X, 1994. 26511
Pope, C. A. and Dockery, D. W.: Health effects of fine particulate air pollution: lines that connect, J. Air Waste Manage., 56, 709–742, doi:10.1080/10473289.2006.10464485, 2006. 26498
Pye, H. O. T., Liao, H., Wu, S., Mickley, L. J., Jacob, D. J., Henze, D. K., and Seinfeld, J. H.: Effect of changes in climate and emissions on future sulfate-nitrate-ammonium aerosol levels in the United States, J. Geophys. Res.-Atmos., 114, D01205, doi:10.1029/2008JD010701, 2009. 26505, 26509
Racherla, P. N. and Adams, P. J.: The response of surface ozone to climate change over the Eastern United States, Atmos. Chem. Phys., 8, 871–885, doi:10.5194/acp-8-871-2008, 2008. 26505
Reich, P. B. and Amundson, R. G.: Ambient levels of ozone reduce net photosynthesis in tree and crop species, Science, 230, 566–570, doi:10.1126/science.230.4725.566, 1985. 26498
Schaub, M. J., Skelly, J., Zhang, J., Ferdinand, J., Savage, J., Stevenson, R., Davis, D., and Steiner, K.: Physiological and foliar symptom response in the crowns of Prunus serotina, Fraxinus americana and Acer rubrum canopy trees to ambient ozone under forest conditions, Science, 133, 553–567, doi:10.1016/j.envpol.2004.06.012, 2005. 26498
Scholze, M., Knorr, W., Arnell, N. W., and Prentice, I. C.: A climate-change risk analysis for world ecosystems, P. Natl. Acad. Sci. USA, 103, 13116–13120, doi:10.1073/pnas.0601816103, 2006. 26510
Sitch, S., Cox, P. M., Collins, W. J., and Huntingford, C.: Indirect radiative forcing of climate change through ozone effects on the land-carbon sink, Nature, 448, 791–794, doi:10.1038/nature06059, 2007. 26498
Spracklen, D. V., Mickley, L. J., Logan., J. A., Hudman, R. C., Yevich, R., Flannigan, M. D., and Westerling, A. L.: Impacts of climate change from 2000 to 2050 on wildfire activity and carbonaceous aerosol concentrations in the western United States, J. Geophys. Res., 114, D2030, doi:10.1029/2008JD010966, 2009. 26497, 26499, 26510
Tagaris, E., Manomaiphiboon, K., Liao, K.-J., Leung, L. R., Woo, J.-H., He, S., Amar, P., and Russell, A. G.: Impacts of global climate change and emissions on regional ozone and fine particulate matter concentrations over the United States, J. Geophys. Res.-Atmos., 112, D14312, doi:10.1029/2006JD008262, 2007. 26509, 26515

ACPD
14, 26495–26543, 2014

Tai, A. P. K., Mickley, L. J., and Jacob, D. J.: Impact of 2000–2050 climate change on fine particulate matter ($PM_{2.5}$) air quality inferred from a multi-model analysis of meteorological modes, Atmos. Chem. Phys., 12, 11329–11337, doi:10.5194/acp-12-11329-2012, 2012. 26504, 26505

Tai, A. P. K., Mickley, L. J., Heald, C. L., and Wu, S.: Effect of CO_2 inhibition on biogenic isoprene emission: implications for air quality under 2000 to 2050 changes in climate, vegetation, and land use, Geophys. Res. Lett., 40, 3479–3483, doi:10.1002/grl.50650, 2013. 26514, 26515

Tai, A. P. K., Val Martin, M., and Heald, C. L.: Threat to future global food security from climate change and ozone air pollution, Nature Climate Change, 4, 817–821, doi:10.1038/nclimate2317, 2014. 26498

Tie, X., Madronich, S., Walters, S., Edwards, D. P., Ginoux, P., Mahowald, N., Zhang, R., Lou, C., and Brasseur, G.: Assessment of the global impact of aerosols on tropospheric oxidants, J. Geophys. Res.-Atmos., 110, D03204, doi:10.1029/2004JD005359, 2005. 26500

US EPA: Guidance for Estimating Natural Visibility Conditions Under the Regional Haze Rule, Tech. Rep. EPA 454/B-03-005, U. S. Environmental Protection Agency Office of Air Quality Planning and Standards Emissions, Monitoring and Analysis Division Air Quality Trends Analysis Group, Research Triangle Park, NC, 2003. 26498, 26511

Val Martin, M., Heald, C. L., Ford, B., Prenni, A. J., and Wiedinmyer, C.: A decadal satellite analysis of the origins and impacts of smoke in Colorado, Atmos. Chem. Phys., 13, 7429–7439, doi:10.5194/acp-13-7429-2013, 2013. 26498

Val Martin, M., Heald, C. L., and Arnold, S. R.: Coupling dry deposition to vegetation phenology in the Community Earth System Model: implications for the simulation of surface O_3, Geophys. Res. Lett., 41, 2988–2996, doi:10.1002/2014GL059651, 2014. 26500, 26503, 26507

van Vuuren, D., Edmonds, J., Kainuma, M., Riahi, K., Thomson, A., Hibbard, K., Hurtt, G., Kram, T., Krey, V., Lamarque, J.-F., Masui, T., Meinshausen, M., Nakicenovic, N., Smith, S., and Rose, S.: The representative concentration pathways: an overview, Climatic Change, 109, 5–31, doi:10.1007/s10584-011-0148-z, 2011. 26501, 26515

Wesely, M.: Parameterization of surface resistances to gaseous dry deposition in regional-scale numerical models, Atmos. Environ., 23, 1293–1304, doi:10.1016/0004-6981(89)90153-4, 1989. 26500, 26507

Wu, S., Mickley, L. J., Jacob, D. J., Rind, D., and Streets, D. G.: Effects of 2000–2050 changes in climate and emissions on global tropospheric ozone and the policy-relevant

ACPD
14, 26495–26543, 2014

background surface ozone in the United States, J. Geophys. Res.-Atmos., 113, D18312, doi:10.1029/2007JD009639, 2008. 26514

Wu, S., Mickley, L. J., Kaplan, J. O., and Jacob, D. J.: Impacts of changes in land use and land cover on atmospheric chemistry and air quality over the 21st century, Atmos. Chem. Phys., 12, 1597–1609, doi:10.5194/acp-12-1597-2012, 2012. 26497, 26506, 26507

Yue, X., Mickley, L. J., Logan, J. A., and Kaplan, J. O.: Ensemble projections of wildfire activity and carbonaceous aerosol concentrations over the western United States in the mid-21st century, Atmos. Environ., 77, 767–780, doi:10.1016/j.atmosenv.2013.06.003, 2013. 26497, 26499, 26510, 26513

ACPD

14, 26495–26543, 2014

Table 1. Summary of main RCP4.5 and RCP8.5 anthropogenic greenhouse gas concentrations and sea-surface temperature (SST) for 2000 and 2050.

Year	Scenario	Concentrations (ppm) CO_2	CH_4	N_2O	SST (°C)
2000	Baseline	367	1760	316	12.2
2050	RCP4.5	487	1833	350	12.6
	RCP8.5	541	2740	367	13.0

ACPD
14, 26495–26543, 2014

Table 2. Anthropogenic short-lived air pollutants and biogenic emissions in 2000 and 2050, projected by the RCP4.5 and RCP8.5 scenarios over the United States.

		Anthropogenic Emissions[a]							Biogenic Emissions[b]	
Year	Scenario	BC	OC	CO	NO_x	NH_3	NMVOCs	SO_2	Isoprene	Monoterpenes
					eastern US					
2000	Baseline	0.29	0.41	70.38	4.82	1.53	1.96	6.30	20.5	6.3
2050	RCP4.5	0.15	0.19	8.70	1.04	1.92	0.90	0.80	33.7	9.4
2050	RCP8.5	0.03	0.06	7.99	1.35	2.21	0.36	0.63	27.8	8.0
					western US					
2000	Baseline	0.10	0.15	25.82	1.58	1.36	0.64	1.77	7.4	2.5
2050	RCP4.5	0.05	0.08	3.55	0.39	1.81	0.30	0.29	9.4	3.0
2050	RCP8.5	0.02	0.03	7.20	0.79	2.16	0.15	0.54	9.6	3.3

[a] Reported Tg C $year^{-1}$ for BC, OC and NMVOCs; Tg N $year^{-1}$ for NO_x and NH_3; Tg S $year^{-1}$ for SO_2; and Tg CO $year^{-1}$ for CO.
[b] Reported Tg C $year^{-1}$.

ACPD
14, 26495–26543, 2014

Table 3. List of simulations[a].

Forcings	2000 Baseline	2050 Total	2050 Climate	2050 Emissions	2050 Land Use
Climate	2000	2050	2050	2000	2000
Emissions[b]:					
Anthropogenic	2000	2050	2000	2050	2000
BB	2000	2050	2000	2050	2000
Biogenic	2000	2050	2000	2000	2050
Land Use[c]	2000	2050	2000	2000	2050

[a] Years represent the year forcing parameter selected for each simulation.
[b] Anthropogenic is the RCP surface and ship emissions, BB is the RCP biomass burning emissions and are considered anthropogenic impact; Biogenic is biogenic emissions calculated by MEGAN v2.1 (see text for further explanation).
[c] Land is the human induced land cover and land use projected by the RCP scenarios.

ACPD
14, 26495–26543, 2014

Table 4. Simulated annual air quality over the US National Parks and wilderness areas[a].

National Park	$PM_{2.5}$ ($\mu g\ m^{-3}$)			MDA-8 O_3 (ppb)			W126 O_3 (ppm h)		
	2000 Base	2050 RCP4.5	2050 RCP8.5	2000 Base	2050 RCP4.5	2050 RCP8.5	2000 Base	2050 RCP4.5	2050 RCP8.5
Acadia, ME (44° N, 68° W)	4.3	2.2	2.2	48.0	43.9	48.8	13.1	2.5	4.7
Arches, UT (39° N, 110° W)	3.2	1.6	2.6	57.8	51.2	60.8	39.9	10.4	39.1
Badlands, SD (44° N, 102° W)	4.1	1.7	3.1	49.4	47.8	55.1	15.9	11.5	29.2
Big Bend, TX (29° N, 103° W)	5.2	2.9	3.8	47.0	42.9	49.4	5.9	2.9	8.5
Biscayne, FL (26° N, 80° W)	5.9	3.9	3.3	45.7	40.4	45.6	1.1	0.5	1.0
Black Canyon, CO (39° N, 108° W)	3.3	1.8	2.8	57.0	50.9	60.4	34.5	8.7	34.6
Bryce Canyon, UT (38° N, 112° W)	4.1	2.1	3.2	58.7	51.7	59.7	45.8	12.1	33.3
Canyonlands, UT (38° N, 110° W)	3.2	1.6	2.6	57.8	51.2	60.8	39.9	10.4	39.1
Capitol Reef, UT (38° N, 111° W)	3.2	1.6	2.6	57.8	51.2	60.8	39.9	10.4	39.1
Carlsbad Caverns, NM (32° N, 104° W)	5.0	2.6	3.2	50.7	45.5	52.3	13.4	4.9	13.1
Channel Islands, CA (34° N, 119° W)	8.6	6.2	5.6	52.4	50.2	55.5	12.2	4.6	9.6
Congaree, SC (34° N, 81° W)	10.2	4.6	4.7	53.6	46.3	52.3	23.4	4.2	11.8
Crater Lake, OR (43° N, 122° W)	4.2	4.2	3.0	50.1	46.6	52.2	11.9	3.1	5.4
Cuyahoga Valley, OH (41° N, 82° W)	15.9	5.8	5.2	53.2	49.0	52.3	61.3	21.7	28.4
Death Valley, CA (36° N, 117° W)	3.4	2.1	2.1	58.9	52.7	58.9	45.5	15.1	28.3
Dry Tortugas, FL (25 N,83 W)	6.0	4.2	4.0	40.8	38.4	44.6	0.6	0.5	1.2
Everglades, FL (25° N, 81° W)	5.9	3.9	3.3	45.7	40.4	45.6	1.1	0.5	1.0
Glacier, MT (49° N, 114° W)	3.1	2.6	2.5	48.5	46.8	52.7	9.5	4.2	9.7
Grand Canyon, AZ (36° N, 113° W)	4.1	2.1	3.2	58.7	51.7	59.7	45.8	12.1	33.3
Grand Teton, WY (44° N, 111° W)	2.2	1.4	1.8	53.8	50.8	58.2	18.1	8.3	22.8
Great Basin, NV (39° N, 114° W)	2.5	1.5	1.7	57.0	51.6	59.0	34.7	11.5	28.2
Great Sand Dunes, CO (38° N, 105° W)	4.2	2.0	3.3	55.9	49.7	59.1	29.7	8.5	32.1
Great Smoky Mountains, NC, TN (36° N, 83° W)	10.9	5.6	4.2	55.7	46.4	51.8	43.8	5.7	14.9
Guadalupe Mountains, TX (32° N, 105° W)	5.0	2.6	3.2	50.7	45.5	52.3	13.4	4.9	13.1
Hot Springs, AR (34° N, 93° W)	10.8	4.7	5.5	53.0	43.9	51.0	32.0	3.9	13.3
Isle Royale, MI (48° N, 88° W)	3.7	2.6	3.0	43.3	42.8	47.7	4.8	2.8	6.5
Joshua Tree, CA (34° N, 116° W)	16.9	13.4	13.9	62.3	53.7	58.4	57.9	20.2	28.2
Kings Canyon, CA (37° N, 118° W)	3.4	2.1	2.1	58.9	52.7	58.9	45.5	15.1	28.3
Lassen Volcanic, CA (40° N, 121° W)	4.7	5.2	3.6	51.2	48.0	54.4	14.0	4.0	9.3
Mammoth Cave, KY (37° N, 86° W)	15.1	6.4	6.2	54.5	46.4	52.4	49.1	7.6	22.6
Mesa Verde, CO (37° N, 108° W)	4.6	2.1	3.9	57.8	50.5	60.6	40.8	8.8	38.6
Mount Rainier, WA (47° N, 122° W)	5.1	3.4	2.6	45.9	43.4	47.8	5.2	1.0	1.6
North Cascades, WA (49° N, 121° W)	4.9	3.2	2.4	45.2	43.3	47.7	6.3	1.2	1.9
Olympic, WA (48° N, 123° W)	4.9	3.2	2.4	45.2	43.3	47.7	6.3	1.2	1.9
Petrified Forest, AZ (35° N, 110° W)	5.5	2.6	4.4	58.2	50.3	59.3	44.0	10.2	34.6
Redwood, CA (41° N, 124° W)	3.4	3.4	2.6	44.9	44.4	49.5	1.2	0.8	1.4
Rocky Mountain, CO (40° N, 106° W)	4.6	2.0	3.1	56.8	51.8	60.0	37.9	13.6	36.4
Saguaro, AZ (32° N, 110° W)	6.1	3.3	4.3	57.8	49.6	56.3	45.0	10.0	23.0
Sequoia, CA (36° N, 119° W)	3.4	2.1	2.1	58.9	52.7	58.9	45.5	15.1	28.3
Shenandoah, VA (38° N, 78° W)	13.2	6.2	4.0	57.0	49.0	51.7	66.5	11.7	13.3
Theodore Roosevelt, ND (47° N, 103° W)	4.8	1.8	3.6	47.8	46.8	53.6	16.2	11.0	29.3
Voyageurs, MN (48° N, 93° W)	4.1	2.3	3.2	43.5	42.9	48.0	5.7	3.0	7.4
Wind Cave, SD (44° N, 103° W)	4.1	1.7	3.1	49.4	47.8	55.1	15.9	11.5	29.2
Yellowstone, WY, MT, ID (45° N, 110° W)	2.2	1.4	1.8	53.8	50.8	58.2	18.1	8.3	22.8
Yosemite, CA (38° N, 119° W)	5.5	3.3	2.7	60.1	52.8	58.5	60.4	18.9	29.1
Zion, UT (37° N, 113° W)	4.1	2.1	3.2	58.7	51.7	59.7	45.8	12.1	33.3

[a] Shown only results for the 46 protected National Parks located in the continental United States; Results from other NPs and wilderness areas can be provided by request.

ACPD
14, 26495–26543, 2014

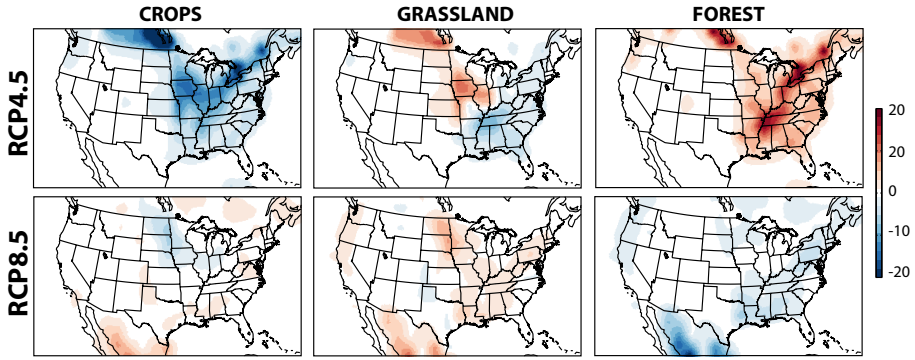

Figure 1. Projected 2050–2000 changes (%) in forest, grasslands and croplands by the RCP4.5 and RCP8.5 scenarios.

ACPD
14, 26495–26543, 2014

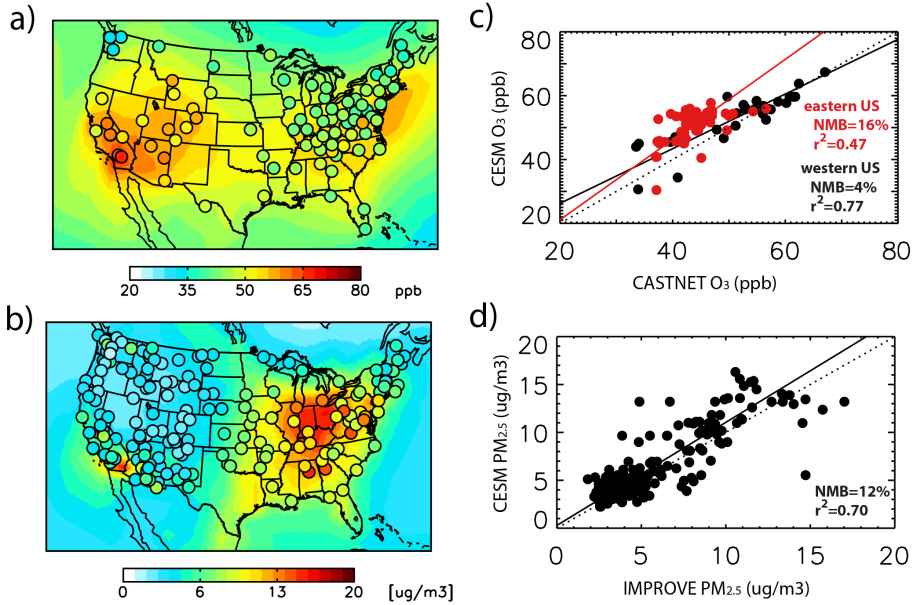

Figure 2. Simulated and observed present-day surface MDA-8 O_3 and $PM_{2.5}$ **(a, b)** and the scatter plots with modeled and observed values at the individual sites **(c, d)**. Observations are long-term means (1998–2010) from the CASTNET and IMPROVE networks. The squared-correlation coefficients (r^2) and normalized mean biases (NMB) are shown in the inset. Reduced-major axis regression lines (solid) and the 1 : 1 lines (dash) are also shown.

ACPD
14, 26495–26543, 2014

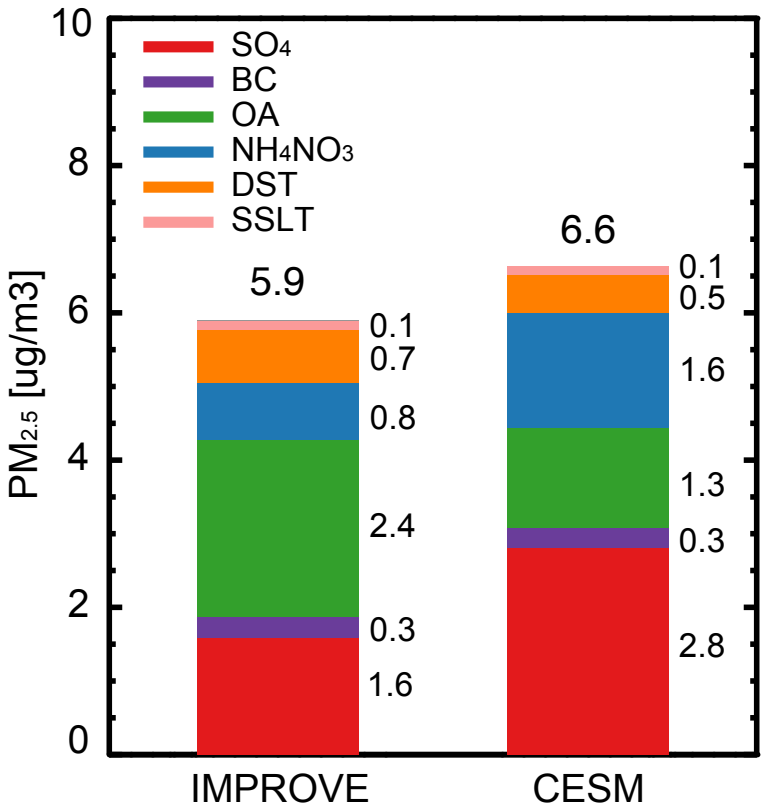

Figure 3. Simulated and observed $PM_{2.5}$ chemical speciation over the United States. Big numerals indicate the annual $PM_{2.5}$ concentrations, whereas small numerals indicate $PM_{2.5}$ chemical species concentrations.

ACPD
14, 26495–26543, 2014

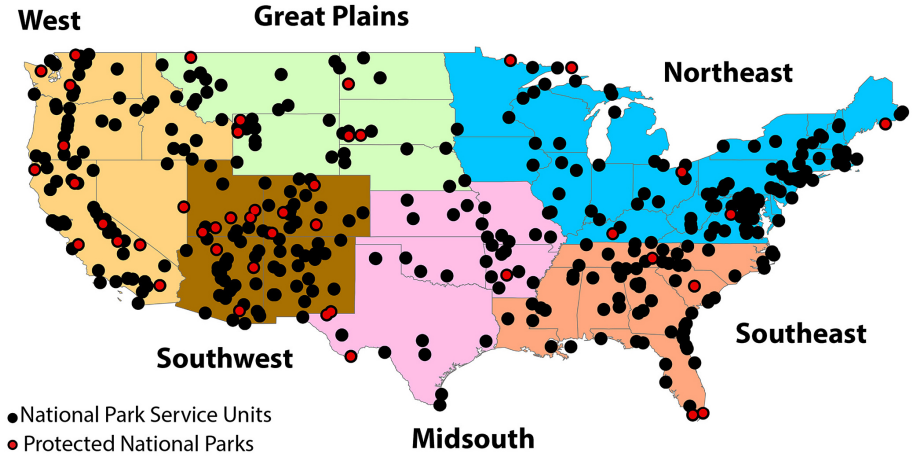

Figure 4. Location of the US National Park units and wilderness areas used in this study. The US protected National Parks are highlighted in red; the six US climatic regions are also identified.

ACPD
14, 26495–26543, 2014

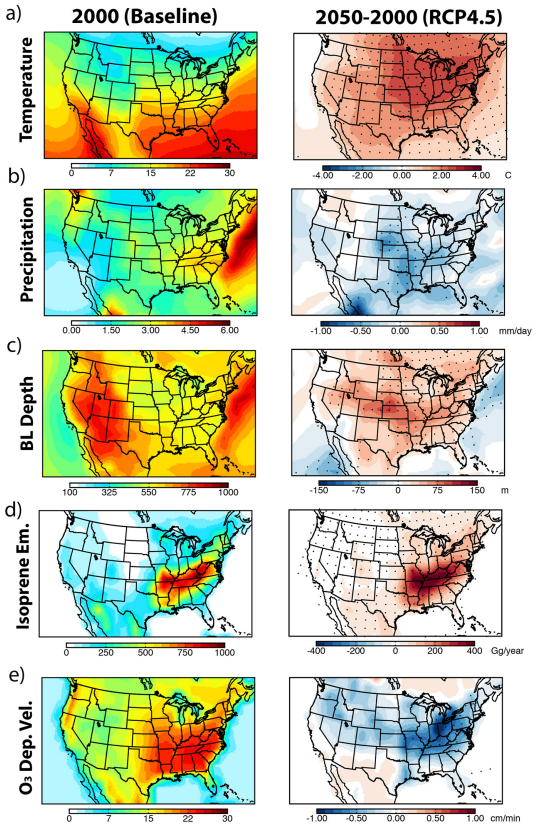

Figure 5. Simulated annual average present-day (left) and projected 2050–2000 changes (right) for surface temperature **(a)**, precipitation **(b)**, boundary layer depth **(c)**, isoprene emissions **(d)** and O_3 dry deposition velocity **(e)**. All maps show changes predicted by the RCP4.5 as a result of the combination of climate, land use and emissions changes, except O_3 dry deposition velocity that shows only land use changes. Regions with changes that are significant at the 95 % confidence level are indicated in the maps with dots.

ACPD
14, 26495–26543, 2014

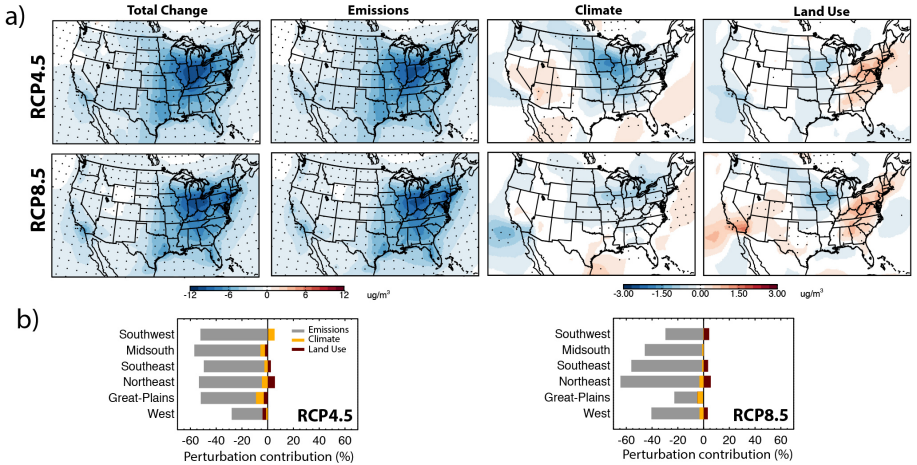

Figure 6. Projected simulated 2050–2000 changes in annual $PM_{2.5}$ as a result of the combination of climate, land use and emissions changes, and the individual changes **(a)**, and the percentage contribution of the individual perturbation **(b)**, for the RCP4.5 and RCP8.5 scenarios. Regions with changes that are significant at the 95 % confidence level are indicated in the maps with dots.

ACPD
14, 26495–26543, 2014

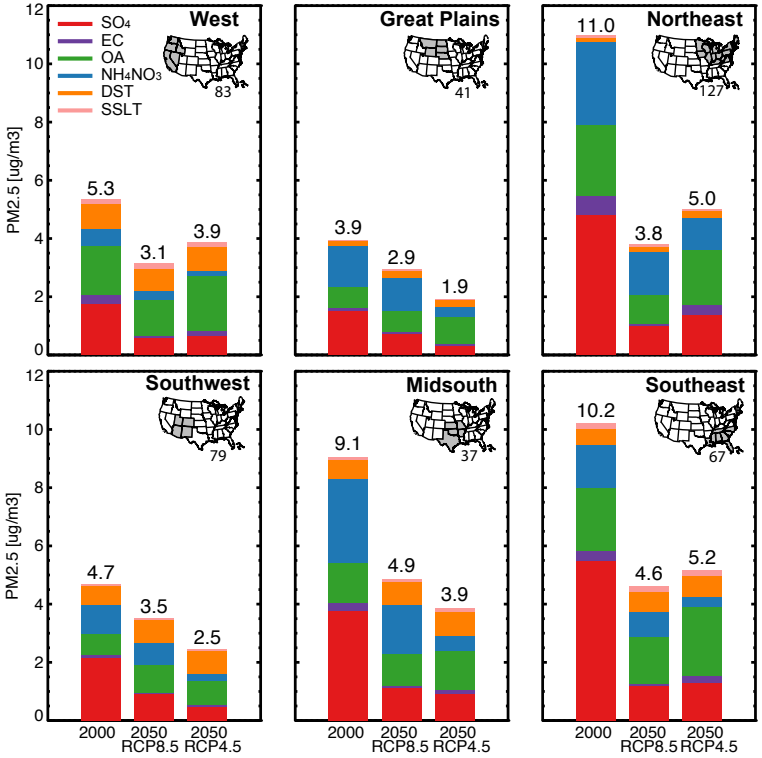

Figure 7. Annual $PM_{2.5}$ chemical speciation for present-day and 2050 as predicted by the RCP4.5 and RCP8.5 scenarios in the US climatic regions. The inset maps show the states in the region in gray, and the numerals indicate the numbers of US National Parks and wilderness areas in each climatic region. Big numerals indicate the annual $PM_{2.5}$ concentrations.

ACPD
14, 26495–26543, 2014

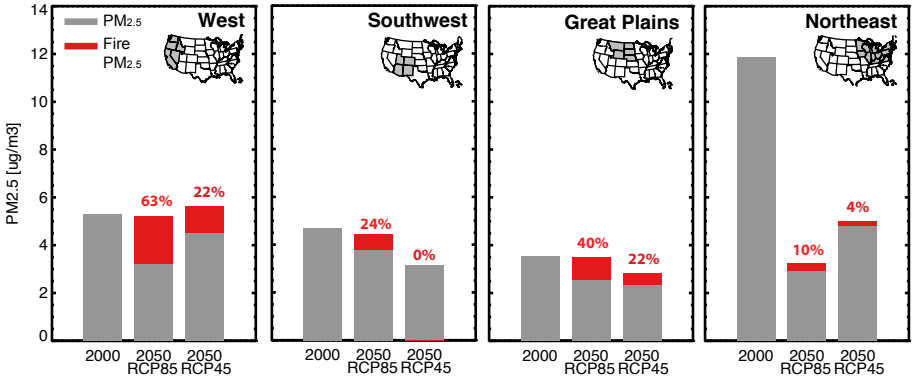

Figure 8. Changes in $PM_{2.5}$ resulting from climate-driven fire activity in the US regions affected by fire. Simulated $PM_{2.5}$ by the RCP scenarios is shown in gray and future $PM_{2.5}$ from climate-driven fire emissions in red. The inset maps show the states in the region in gray and the red numerals indicate the percentage change in $PM_{2.5}$ when climate-driven fire activity is included in the simulation.

ACPD
14, 26495–26543, 2014

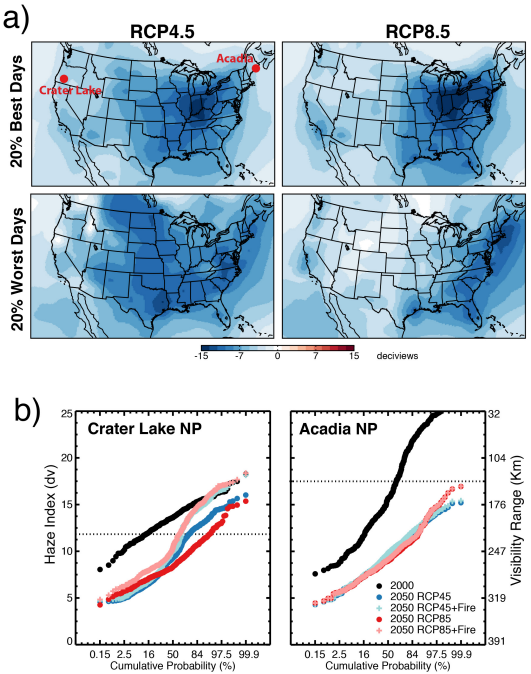

Figure 9. Projected simulated 2050–2000 changes in haze index (HI) as a result of the combination of climate, land use and emissions changes **(a)** and the cumulative probability distributions of daily mean haze index in the Crater Lake and Acadia NPs **(b)**. The maps show "20 % Best Days" as the averaged HI during the cleanest days and "20 % Worst Days" as averaged HI during the haziest days (see text for further explanation). The location of the Crater Lake and Acadia NPs are indicated in the top left map. The cumulative distribution plots show simulated daily HI for present-day (black circles), 2050 projected by RCP4.5 (blue circles) and by RCP8.5 (red circles), and 2050 with the effects of climate-driven fires by RCP4.5 (light blue cross) and by RCP8.5 (light red cross). The 2050 HI target to reach natural visibility conditions by 2064 are indicated with a horizontal dotted line.

ACPD
14, 26495–26543, 2014

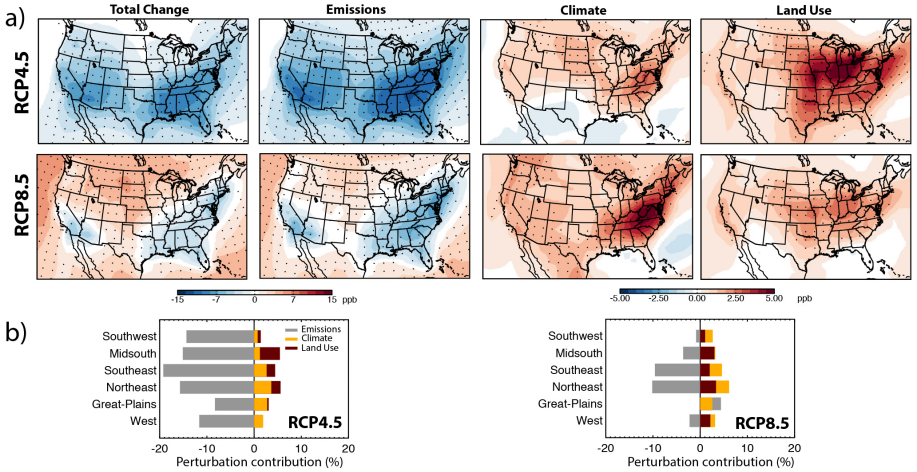

Figure 10. Projected simulated 2050–2000 changes in surface O_3 as a result of the combination of climate, land use and emissions changes, and the individual changes **(a)** and the percentage contribution of the individual perturbations **(b)**, for the RCP4.5 and RCP8.5 scenarios. Regions with changes that are significant at the 95 % confidence level are indicated in the maps with dots, and O_3 concentrations are annual maximum daily 8 h (MDA-8) averages.

ACPD
14, 26495–26543, 2014

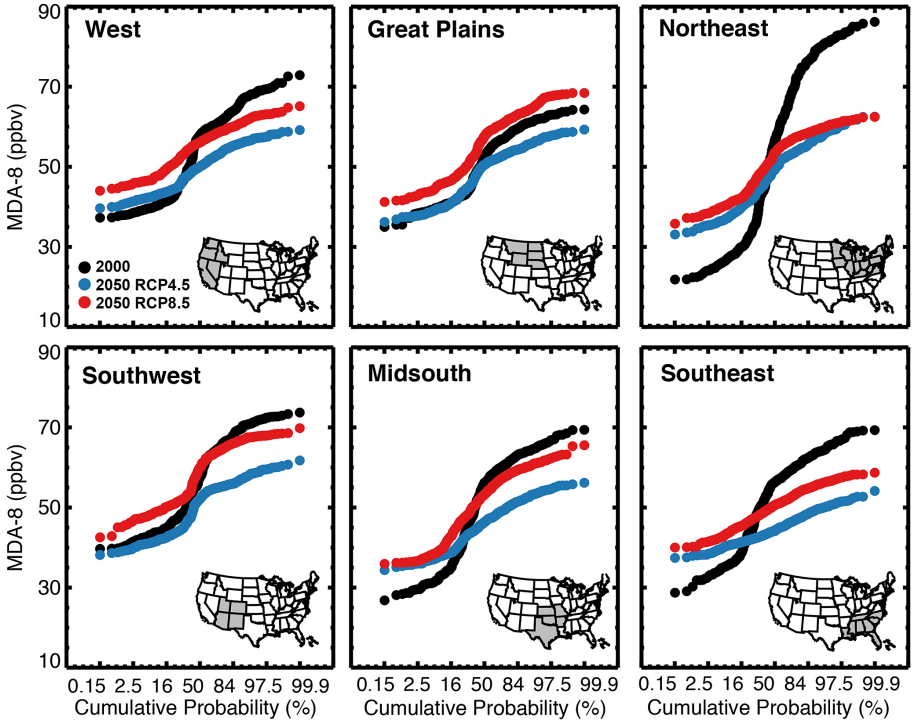

Figure 11. Cumulative probability distributions of simulated surface O_3 MDA-8 averaged over the US National Parks and wilderness areas in the US climatic regions, for present-day (black circles) and 2050 predicted by the RCP4.5 (blue circles) and RCP8.5 (red circles) scenarios. The inset maps show the states in the region in gray.

ACPD
14, 26495–26543, 2014

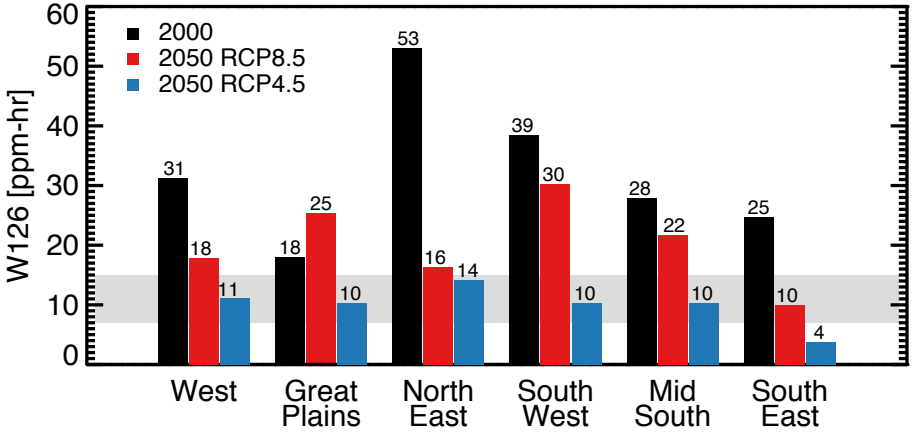

Figure 12. Simulated summertime W126 O_3 in 2000 (black) and 2050 RCP4.5 (blue) and RCP8.5 (red) averaged over the US climatic regions. Numerals indicate the simulated O_3 W126 value, and grey shaded area represent the minimum and maximum recommended standard (7–15 ppm h).

ACPD
14, 26495–26543, 2014